



Biosensors for melanoma skin cancer diagnostics

Eleni Chatzilakou^a, Yubing Hu^{a,***}, Nan Jiang^{b,c,**}, Ali K. Yetisen^{a,*}

^a Department of Chemical Engineering, Imperial College London, South Kensington, London, SW7 2BU, UK

^b West China School of Basic Medical Sciences & Forensic Medicine, Sichuan University, Chengdu, 610041, China

^c JinFeng Laboratory, Chongqing, 401329, China



ARTICLE INFO

Keywords:

Skin cancer

Melanoma

Biosensors

Diagnostic tools

Early detection

ABSTRACT

Skin cancer is a critical global public health concern, with melanoma being the deadliest variant, correlated to 80% of skin cancer-related deaths and a remarkable propensity to metastasize. Despite notable progress in skin cancer prevention and diagnosis, the limitations of existing methods accentuate the demand for precise diagnostic tools. Biosensors have emerged as valuable clinical tools, enabling rapid and reliable point-of-care (POC) testing of skin cancer. This review offers insights into skin cancer development, highlights essential cutaneous melanoma biomarkers, and assesses the current landscape of biosensing technologies for diagnosis. The comprehensive analysis in this review underscores the transformative potential of biosensors in revolutionizing melanoma skin cancer diagnosis, emphasizing their critical role in advancing patient outcomes and healthcare efficiency. The increasing availability of these approaches supports direct diagnosis and aims to reduce the reliance on biopsies, enhancing POC diagnosis. Recent advancements in biosensors for skin cancer diagnosis hold great promise, with their integration into healthcare expected to enhance early detection accuracy and reliability, thereby mitigating socioeconomic disparities.

1. Introduction

Skin cancer, a globally prevalent malignancy, has seen a significant increase in incidence since the late 20th century. In 2020, over 1.5 million skin cancer cases were diagnosed, with projections indicating a rise to over 2.3 million by 2040. Ultraviolet (UV) radiation, driven by stratospheric ozone changes and climate shifts, stands as the primary cause of most skin cancer cases (D'Orazio et al., 2013). Non-melanoma skin cancers, predominantly Basal Cell Carcinoma (BCC) and Squamous Cell Carcinoma (SCC), are relatively less aggressive. However, cutaneous melanoma, though less common, is highly dangerous, accounting for 80% of skin cancer deaths and posing a substantial metastatic risk (Davis et al., 2019).

Scientific advancements, such as the introduction of dermoscopy and computer-assisted diagnostic tools, have improved our understanding of skin tumours. These developments span from the 1980s, when early melanoma detection efforts began, to the creation of devices like the MoleMax (DermaMedical Systems, Vienna, Austria) and MelaFind (Electro-Optical Sciences, Irvington, NY) in the 1990s (Fig. 1)

(Gutkowicz-Krusin et al., 2000; Young et al., 2021). Multispectral technology and algorithmic integration came in the 2000s, with real-time imaging techniques like ultrasound, confocal microscopy, and bioimpedance contributing since 2005 (Aberg et al., 2004; Carrara et al., 2007; Rigel et al., 2010). Additionally, tape-stripping techniques and smartphone apps have further advanced melanoma screening (Wong et al., 2006). The last decade has witnessed the combination of previously invented technologies, producing integrated systems like Vectra WB360 (Canfield Scientific, USA) and MoleSafe (MoleSafe™, USA) (Rayner et al., 2018). Moreover, AI, machine learning, and computer vision have demonstrated promise in enhancing melanoma diagnostics, though access to substantial data pipelines remains a challenge for clinical-grade AI (Atkins et al., 2021; Schlessinger et al., 2019; Tschanl et al., 2019; Waldman et al., 2021; Young et al., 2020). Studies have highlighted convolutional neural networks' (CNNs) effectiveness in binary image classification of skin neoplasms, including melanoma and keratinocyte cancers (Han et al., 2018). CNNs consistently match or surpass expert clinicians in performance yet their transition to real-world clinical settings is ongoing (Atkins et al., 2021). The skin

* Corresponding author.

** Corresponding author. West China School of Basic Medical Sciences & Forensic Medicine, Sichuan University, Chengdu, 610041, China.

*** Corresponding author.

E-mail addresses: yubing.hu@imperial.ac.uk (Y. Hu), jiangnansophia@scu.edu.cn (N. Jiang), a.yetisen@imperial.ac.uk (A.K. Yetisen).

cancer diagnostics market shows significant growth, driven by increased awareness and product launches projected to reach \$5.5 Bn (2028) (The Insight Partners, 2022a, b).

The established advancements, while beneficial, are associated with drawbacks including increased cost and erratic patient compliance

limiting their utilization in benchtop applications within research environments (Young et al., 2021). Bio-cybersecurity and bioethics are critical aspects of any tool or application involving the acquisition and processing of patient data and before their extensive implementation, an inclusive legal frame should be formed. Their role as clinical

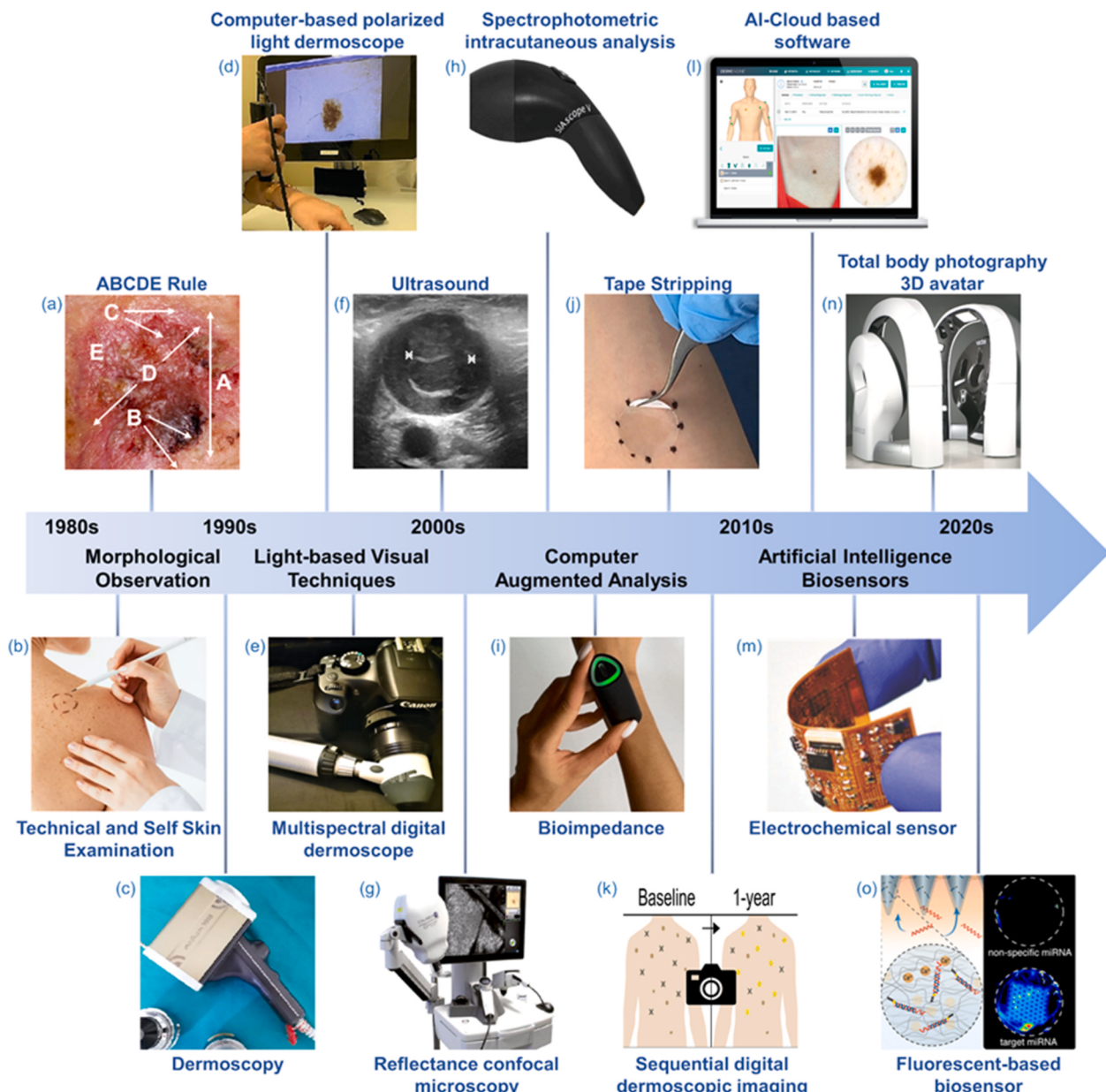


Fig. 1. The timeline of diagnostic technologies that have contributed to the prevention and diagnosis of skin cancers, including melanoma. A range of non-invasive imaging techniques has been developed, from using hand-held dermatoscopes in the 1990s to the more recent bioimpedance-based devices in 2021, enhancing diagnostic accuracy. The past decade witnessed the combinational development of previously invented technologies and leveraging artificial intelligence to facilitate diagnosis, while the state-of-the-art devices are primarily biosensors. (a) The ABCDE rule for evaluation of suspicious areas (Thompson, 2023). Copyright © Attribution 4.0 International (CC BY 4.0), contributor Geraldine Thompson. (b) Technical and self-skin evaluation (Kensington International Clinic, 2023). Copyright © Kensington International Clinic (Google Creative Common Licenses). (c) Hand-held dermoscope Tognetti et al., (2020); Copyright © 2020 Springer Nature Switzerland AG. (d) Computer-based polarized light dermoscope Tognetti et al., (2020); Springer Nature Switzerland AG. (e) Portable dermoscope-camera systems Tognetti et al., (2020); Copyright © 2020 Springer Nature Switzerland AG. (f) Melanoma in lymph nodes (Mim, 2018). Copyright © Wikimedia Commons (CC BY-SA 4.0), contributor Mme Mim. (g) Confocal microscope VivaScope 1500 (Malvehy and Pellacani, 2017). Copyright © Acta Dermato-Venerologica (CC BY-NC 4.0). (h) SIAscope, a melanoma screening device (Wikipedia). Copyright © Wikimedia Common, public domain (PD). (i) NOTA mole tracker (Artes Electronics PTE LTD, 2023). Copyright © obtained from Vassiliy Zotov, CEO Artes Electronic. (j) Tape stripping Hughes et al., (2021); Copyright © 2020 Hughes et al. British Journal of Dermatology, John Wiley & Sons Ltd. (k) Sequential digital dermoscopic imaging (Tschandl, 2018). Copyright © 2018 Tschandl (Reproduced under terms of the CC-BY license). (l) DermEngine, an intelligent dermatology software (MetaOptima Technology Inc., 2023). Copyright © obtained from Maryam Sadeghi, CEO MetaOptima Technology Inc. (m) Sensor for epidermal melanoma screening Ciui et al., (2018); Copyright © 2018 WILEY-VCH. (n) VECTRA WB360, Canfield Scientific, Inc (Canfield Scientific Inc., 2023). Copyright © obtained from Thomas Bialoglow. (o) Microneedle arrays for sensing of circulating nucleic acids Al Sulaiman et al., (2019); Copyright © 2019 American Chemical Society.

decision-support tools is pivotal, but biopsies often remain necessary for definitive diagnoses (Freeman et al., 2020). Biopsies, while effective, carry drawbacks like cost, discomfort, and potential complications. The gold standard of skin biopsy is associated with excessive cost, painful patient discomfort, labour intensity, restricted suitability, infection risk near the perforated location, and wound dehiscence, necessitating the development of accurate, quantifiable and non-invasive diagnostic tools (Linares et al., 2015).

Biosensing technologies, when integrated with existing diagnostic tools, offer the potential for efficient, low-cost, and highly specific POC tests for early skin cancer detection. The global POC diagnostic biosensors market is projected to reach \$25 billion by 2030, with biosensors advancing significantly due to nanotechnology (Strategic Market Search, 2022). These biosensing techniques reduce the need for biopsies, enhance precision, and allow for early diagnosis, even as wearable devices. Examples include microneedle bandage sensors and hydrogel-coated microneedle patches for biomarker sampling (Al Sulaiman et al., 2019; Ciui et al., 2018).

This article serves as a comprehensive resource for researchers and clinicians in the field, exploring the latest advances in skin cancer biosensing technologies and diagnostic biomarkers. It aims to identify knowledge gaps and foster the development of more precise, efficient, and cost-effective diagnostic tools. It uniquely bridges the gap between traditional diagnostic methods and cutting-edge biosensing applications, highlighting the urgent need for seamless integration of these technologies into clinical practice. By identifying knowledge gaps and fostering the development of more precise, efficient, and cost-effective diagnostic tools, this review not only informs but also catalyzes innovation in the field. The review covers benchtop and portable biosensing technologies, including the detection of malignant melanoma signalling proteins and nucleic acids, making it a valuable resource for those seeking the most recent developments in melanoma skin cancer diagnosis.

2. Skin cancer

2.1. Development of cutaneous melanoma

Cutaneous melanoma results from mutations in pigment-producing cells present in the base of the epidermis which results in uncontrolled cellular proliferation and malignant tumour formation. Due to its propensity to rapidly metastasize to other organs when not promptly addressed, it represents the most severe and life-threatening manifestation of skin cancer (Saginala et al., 2021). The four major histological subtypes of cutaneous melanoma are “superficial spreading, nodular, lentigo maligna, and acral lentiginous melanoma” (D’Orazio et al., 2013), corresponding to 70%, 5%, 4 – 15%, 2–5% respectively of the reported cases (Linares et al., 2015). The most commonly used system to stage melanoma has been introduced by the “American Joint Committee on Cancer (AJCC)” and focuses on the tumour, nodes, and metastasis basis outlining five stages (Fig. 2) (Borsari and Longo, 2017). In stages 0-II diagnostic biomarkers are used to confirm the presence and type of the disease, while after a confirmed diagnosis in more progressed stages (II-IV), prognostic biomarkers provide information on the patient’s likely outcome. Prognostic biomarkers are evaluated before treatment and help to identify tumour-specific molecular or histopathological characteristics. The overall formation of the diagnosis is dependent on the following clinically relevant factors: thickness, ulceration, mitotic rate, serum levels of lactate dehydrogenase (LDH), tumour-infiltrating lymphocytes, vertical growth phase, and regression, thus evaluating the level of aggressiveness, the possibility of metastasis or effective immune response.

2.2. Epidemiological statistics

The prevalence of skin cancer has increased significantly since the end of the 20th century. Data published by the WHO state that internationally in 2020 more than 1.5 million skin cancer cases were reported and more than 120,000 deaths were attributed to skin cancer (Fig. 3)

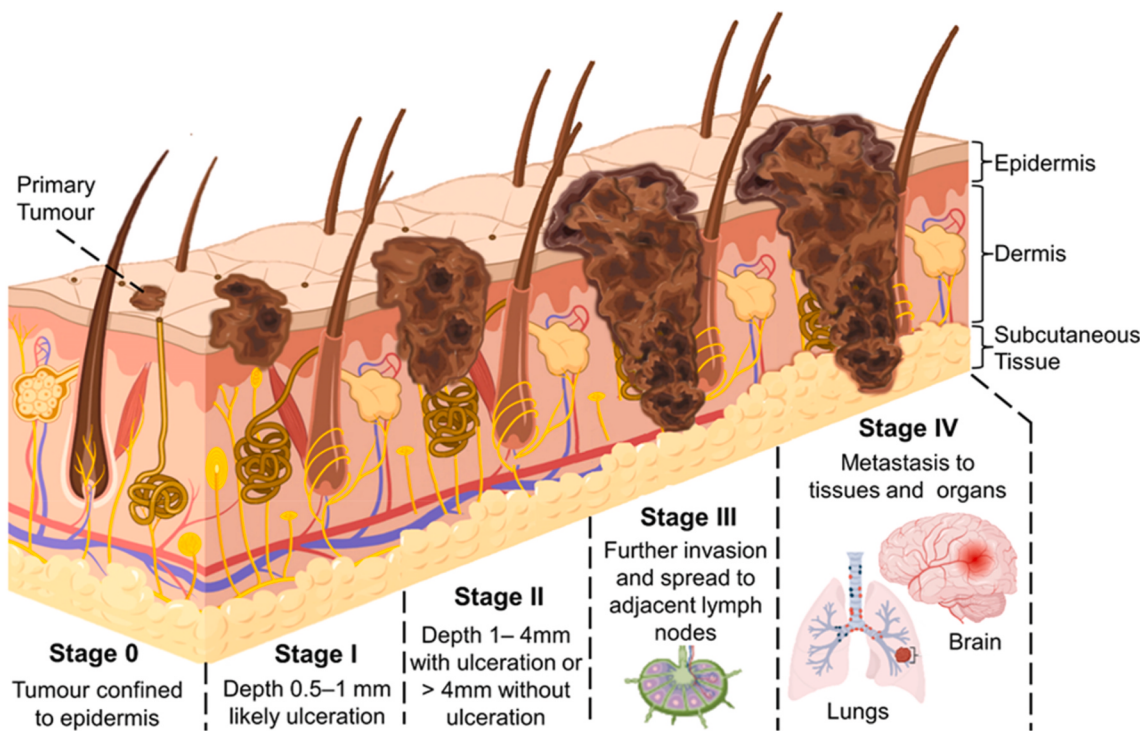


Fig. 2. Schematic illustration of skin cancer progression in different skin layers. Stages 0-I of melanoma are limited to the epidermis, with stage II being thicker and extending into the dermis. Stage III indicates evolution further into the dermis while spreading to nearby lymph nodes and stage IV is metastasis to other parts of the body.

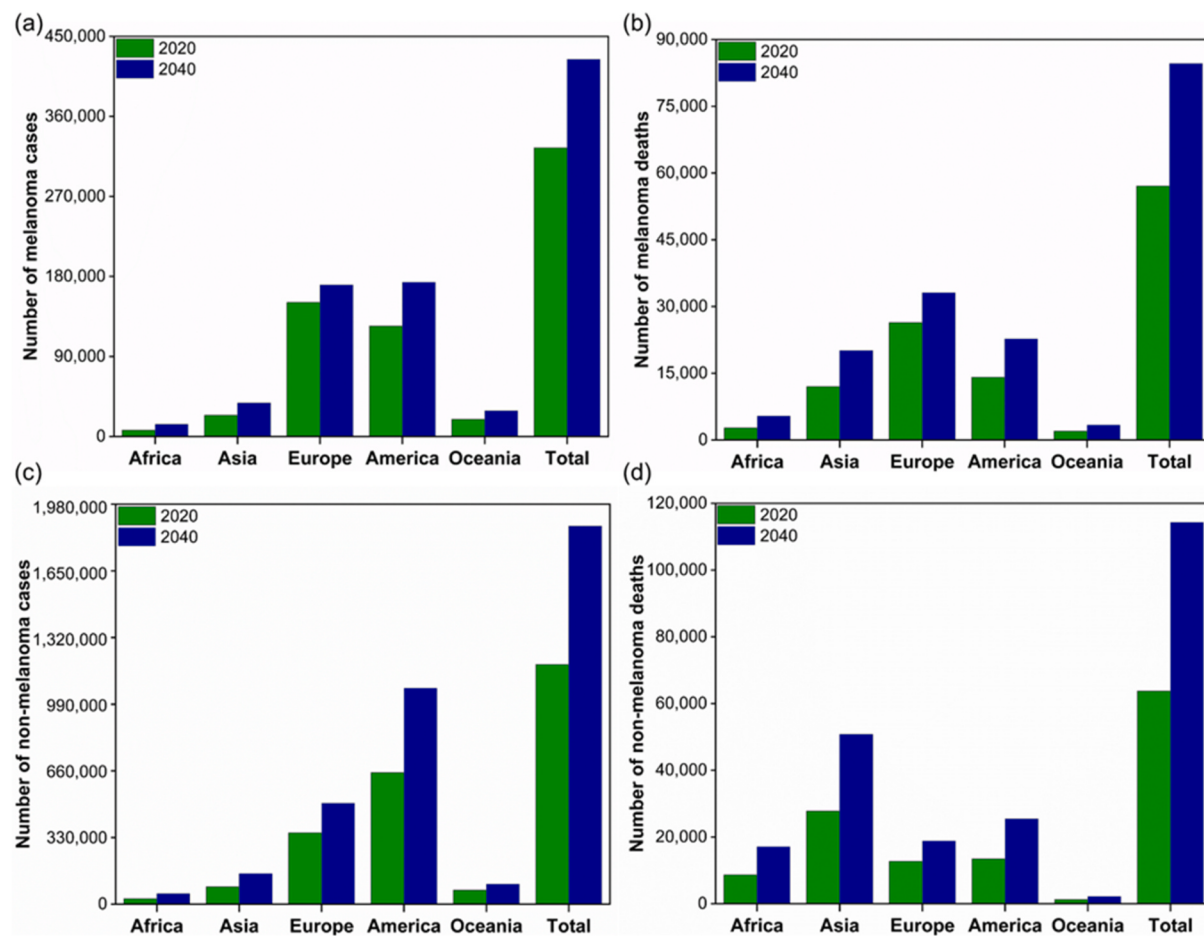


Fig. 3. Increasing skin cancer incidence and mortality rates in 2020 and 2040: (a) The number of annual melanoma skin cancer cases and (b) deaths worldwide. (c) The number of annual non-melanoma skin cancer cases and (d) deaths worldwide. Data was acquired from the World Health Organization ([World Health Organization, 2020](#)). Copyright © International Agency for Research on Cancer (IARC), 2022. All Rights Reserved.

([World Health Organization, 2020](#)). In 2040, the mortality is estimated to increase by 65%, and the total number of skin cancer cases to surpass 2.3 million worldwide. Although the overall 5-year survival of melanoma has risen to 90.5% in the US, survival for disease stages III and IV remains only 60.3 and 16.2%, respectively, with an estimated 48% increase in global mortality by 2040 ([National Cancer Institute, 2022](#); [World Health Organization, 2020](#)).

Caucasians face elevated risk due to limited melanin protection against sun exposure ([Narayananamurthy et al., 2018](#)). In the US, melanoma incidence varies by race/ethnicity. Non-Hispanic Whites have the highest rate at 26 per 100,000, compared to lower rates in Native Americans/Alaskan Natives (7.4), Hispanics (4.6), Asians (1.3), and non-Hispanic Blacks (1.0) ([American Cancer Society, 2023](#); [Harvey et al., 2014](#)). However, Black and Native American patients often present melanoma at later stages, and Asian Americans and Pacific Islanders show adverse indicators at diagnosis, including lymph node involvement ([Fahmy et al., 2023](#)). These disparities intensified from 2000 to 2010 and beyond, despite screening protocol improvements and immunotherapy advances. Socioeconomic and genetic factors, along with differences in tumour proliferation (high ki-67 expression), cell cycle regulation (low-level p53 staining), and angiogenesis, contribute to variations in disease manifestation and prognosis ([Shao and Feng, 2022](#)).

3. Biosensors for diagnostics

3.1. Foundations and principles of biosensing

Melanoma misdiagnosis is responsible for more malpractice and misdiagnosis claims than any other malignancy, second only to breast cancer, while early misdiagnosis drastically reduces a patient's likelihood of survival ([Eftekhari et al., 2019](#)). The importance of developing precise, quantitative, early and decisive skin cancer diagnostic tools is highlighted by the inadequacy of the current means to considerably reduce the mortality rate of skin cancer and enhance early verified diagnosis ([McQuade et al., 2018](#)). In pursuit of this, the currently available indicative tools could be integrated with biosensing technologies for locating problematic areas and identifying biomarkers with suitable innovative bioreceptors, holding the potential to be used as point-of-care (POC), effective, highly specific, and affordable diagnostic modalities.

Biosensors for skin cancer detection are composed of a recognition element in very close spatial proximity with a physical transduction element. Thus, as analytical devices for skin cancer diagnostics, biosensors consist of three fundamental components: (i) the detector, responsible for sensing the stimulus or the biological component specific to skin cancer (biorecognition); (ii) the transducer, which transforms the skin cancer-related stimulus in an output signal (signalization); and (iii) the signal processing system that quantifies the output signal ([Nagel et al., 1992](#)) (Fig. 4).

Bioreceptors, which are mainly immobilized biological systems, are

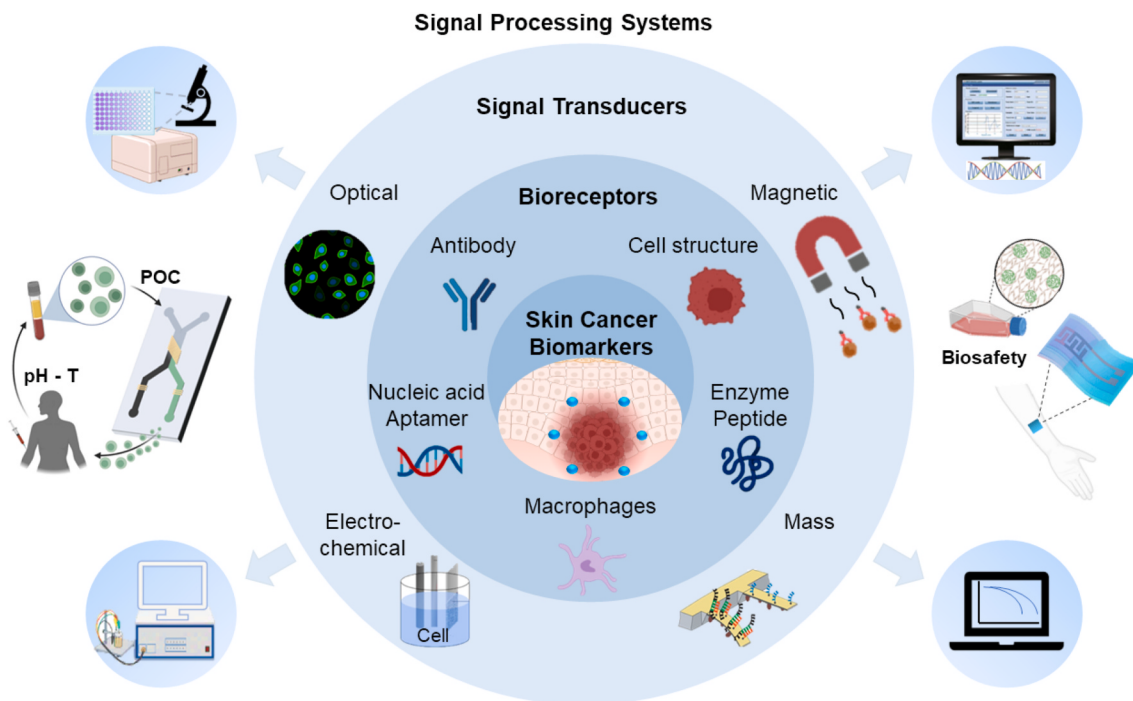


Fig. 4. Overview of biosensor technology for safe and effective skin cancer biomarker detection, showcasing bioreceptors, signal transducers and processors. Mass element Huber et al., (2013); Copyright © 2013 Nature Publishing Group. Computer Element © 2020 Elsevier B.V. All rights reserved.

bonded to the surface of the transducer and are responsible for the identification and specific capturing of the analyte, as well as the physical-chemical mechanism that will generate the signal. Bioreceptors determine the level of specificity of the biosensors and are classified into four major categories “antibodies, enzymes, nucleic acids, and cellular structures” (Naresh and Lee, 2021). Further bioreceptors, such as aptamers, ribonucleic acids, peptides, and macrophages, are progressively being integrated into the context of skin cancer detection.

Antibodies are widely used in biosensors for their high specificity and affinity in antibody-antigen interactions, particularly relevant in identifying skin cancer biomarkers, but face challenges in long-term stability and manufacturing costs, particularly in multi-target applications (Rasooly and Herold, 2009). Enzymatic biosensors offer advantages like high sensitivity and direct visualization, which is crucial in the early detection of skin cancer, though their use as bioreceptors can be complicated by interference from endogenous enzymes (Bucur et al., 2021; Velusamy et al., 2010). Nucleic acid biosensors use strands as bioreceptors for target analytes through complementary base pairing, offering stability and selectivity with rapid, reversible responses, making them suitable for detecting genetic mutations associated with skin cancer, but face challenges of irreversible DNA damage affecting replication and signal amplification (Liu et al., 2019; Perumal and Hashim, 2014; Vo-Dinh and Cullum, 2000). Cell-based biosensors, utilizing live cells as bioreceptors, offer benefits such as non-invasive monitoring and rapid response, valuable for ongoing monitoring of skin cancer progression, yet their effectiveness is limited by factors affecting cell viability, including cell lifespan and sterilization methods (Ziegler, 2000).

The four major categories of biosensors according to the transduction techniques they employ are mass, electrochemical, magnetic, and optical, each with potential applications in skin cancer detection (Bhalla et al., 2016). These techniques are further classified and referred to as direct recognition methods when biosensors take direct advantage of the phenomenon occurring on the transducer surface (i.e., label-free) or indirect when the detection is enhanced by secondary elements, such as fluorophores (Heineman and Jensen, 2006). Recently, scientists have incorporated nanomaterials and nanoparticles in the transduction

process to further improve biosensing properties such as sensitivity, response time, and reproducibility in skin cancer diagnostics (Malekzad et al., 2017).

Mass transducers in biosensors use vibrating piezoelectric crystals to detect mass changes on their surface, offering real-time, label-free detection but facing issues with specificity and interference which can be critical in the accurate detection of skin cancer markers. Electrochemical biosensors, categorized into amperometric, potentiometric, or impedimetric based on the measured parameter, are known for their sensitivity and cost-effectiveness but suffer from signal drift in long-term use especially when used for continuous monitoring of skin cancer biomarkers (Bakker and Telting-Diaz, 2002; Kim et al., 2019). Optical-based biosensors, utilizing various techniques like fluorescence, chemiluminescence, and surface-enhanced Raman spectroscopy (SERS), are widely used for their high sensitivity and specificity, though they face challenges such as photobleaching in fluorescence and the need for excellent bioreceptor immobilization in colourimetry which are significant considerations in the development of optical biosensors for skin cancer (Perez-Jimenez et al., 2020; Qi and Zhang, 2020; Tainaka et al., 2010; Yetisen et al., 2019).

3.2. Biosensor design and safety for skin cancer

Biosensors for skin cancer diagnostics represent a promising area, demanding careful design strategies to ensure adaptability, precision, and compatibility with the skin's unique environment (Rodrigues et al., 2020). Crucial factors such as pH, temperature, and salinity vary significantly across different skin layers and biological fluids, affecting biomolecule behaviour and sensor performance (Zucolotto, 2020). This necessitates the use of non-invasive or minimally invasive sampling methods like interstitial fluid (ISF) sampling to minimize biological system perturbations. Point-of-care (POC) systems are particularly advantageous in skin cancer diagnostics due to their ability for miniaturization and integration of automated sample pre-treatment, enhancing robustness against unsolicited components in biological fluids (Lichtenberg et al., 2019) (Fig. 4).

The development of these biosensors involves optimizing

bioreceptor selectivity to reduce non-specific interactions and enhance binding efficiency with relevant biomarkers (Lichtenberg et al., 2019). Biofouling, resulting from unspecific biomolecule adsorption and the formation of biofluid and microorganism layers, poses a significant challenge, potentially impairing sensor reliability (Liu, 2021). Innovative solutions such as perm-selective protective polymeric coatings are being explored to mitigate these effects by excluding macromolecules and controlling device exposure (Wisniewski and Reichert, 2000).

Moreover, the choice of transducer is pivotal for achieving high sensitivity and selectivity in detecting a range of analytes relevant to skin cancer, such as nucleic acids, metabolites, and proteins. Electrochemical transducers are increasingly favoured in this context (Bakker and Telting-Diaz, 2002). For effective real-time monitoring and diagnosis, advanced reporting methods like smartphone integration and portable spectrometers are being utilized, offering accurate, quantitative measurements in a cost-effective and user-friendly format (Zhang et al., 2022b).

Skin-integrated wearable and implantable biosensor devices, designed to be flexible, lightweight, and ultra-thin, are crucial for comfortable skin movement accommodation and adaptation to the 3D shape of organs (Gray et al., 2018). The substrate materials for biosensors, such as polymers, carbon-based materials, and metal oxides, are chosen for their flexibility, biocompatibility, and large surface area, ensuring minimal immune response and optimal interaction with the biological system (Abu Owida, 2022). Such design considerations ensure that biosensors for skin cancer diagnosis not only meet the clinical requirements but also align with patient comfort and usability.

The direct interface of biosensing technologies with the human body necessitates a rigorous and thorough evaluation of their safety profile. Essential to this evaluation is the identification and mitigation of potential risks, including skin irritation, allergic reactions, and unforeseen long-term effects. It is imperative that these biosensors undergo comprehensive safety assessments, which should encompass dermatological testing for biocompatibility and hypersensitivity reactions. This testing regime must adhere to stringent regulatory standards and ethical guidelines to ensure patient welfare.

Furthermore, the materials and chemicals used in biosensor construction demand careful selection to minimize adverse reactions. Biocompatible and hypoallergenic substances should be prioritized to reduce the likelihood of immunological responses or skin irritation. Continuous monitoring during clinical application is also crucial for early detection and management of any adverse effects. This vigilance allows for the immediate adaptation of the biosensing technology, ensuring ongoing patient safety and comfort.

4. Skin cancer biomarkers

The deployment of biosensors for skin cancer diagnosis requires access to fluids proper for detecting biomarkers. Given their abundance, diagnostic capabilities, and simple sample extraction, readily available bodily fluids, including saliva, sweat, blood, and urine, have been employed for non- or minimally-invasive sampling. Throughout the pursuit of the most effective biomolecules for disease onset and progression, serologic biomarkers have gained attention in melanoma research (Belter et al., 2017). Nevertheless, skin melanoma biomarkers are predominantly present within the melanocytes, in the extracellular fluid surrounding them, or in ISF (Madden et al., 2020; Senf et al., 2020). The abundance of ISF volumetrically in the epidermis, dermis, and subcutaneous tissue is approximately 15–35%, 40%, and 20% respectively (Groenendaal et al., 2010). Interstitial fluid contains almost all analytes present in the blood, including RNA species and circulating proteins, with over 90% of proteins shared between blood and ISF (Friedel et al., 2023). Furthermore, skin ISF contains approximately 83% of the proteins present in serum, but approximately 50% of proteins present in ISF cannot be found in serum, suggesting that unique and common biomarkers can be detected in ISF (Samant and Prausnitz,

2018). ISF can be sampled painlessly and with minimal risk of blood contamination and requires no prior treatment for biomarker analysis.

Biomarkers for skin cancer fall into three categories: diagnostic markers for initial screening, prognostic indicators for monitoring disease progression after diagnosis, and predictive markers that can forecast treatment outcomes (Weinstein et al., 2014). However, this classification lacks clarity as the profiles and applicability of these biomarkers have not been comprehensively analysed yet. Premelanosome protein (PMEL) (else gp100), Melan-A (else MART-1), tyrosinase, MITF, and s100, as well as several recently reported biomarkers, are among those being considered for melanoma diagnosis (Table 1) (Weinstein et al., 2014). Apart from conventionally deployed immunohistochemical assays, recently developed detection methods of diagnostic and prognostic biomarkers utilize novel techniques based on biosensing principles, such as the *in situ* fluorescent hybridization of ribonucleic acids, the detection of enzymatic activities and antigen-antibody interactions. Nevertheless, a combination of biomarkers may be required to distinguish melanoma from melanocytic nevi, as melanoma may acquire several different mutations as it progresses toward cancer (Trager et al., 2022). Thus, mutation combinations that upregulate or downregulate specific genes may prove more consistent with a tangible diagnosis.

4.1. Proteins and enzymes

4.1.1. Cell surface proteins

Cell surface biomarkers can be useful for biosensing technologies meant for the diagnosis of cutaneous melanoma, since they can offer specific and reliable information about the characteristics of melanoma cells and enable the identification of circulating tumour cells (CTCs).

PMEL is a nonmutated antigen expressed in most melanoma and healthy skin cells (Zhang et al., 2021). PMEL has been detected in blood by mass spectrophotometry (The Human Protein Atlas, 2022c) and is over-expressed at all stages of skin cancer, with low expression in tissues other than the skin. Another melanocytic membrane protein is the Melan-A (else known as MART-1; melanoma antigen recognized by T-cells-1), located in organoids of melanocytes (Weinstein et al., 2014), without yet having been detected in blood or serum (The Human Protein Atlas, 2022a). Also, Melan-A is essential for the expression, stability, trafficking, and processing of the PMEL protein, nonetheless, its presence in benign nevi, renders it a marker of histogenesis rather than malignancy (Weedon, 2010). Melanocortin 1 receptor (MC1R) is the receptor of two melanocortin peptides, hence is commonly combined with radiopeptide tumour targeting methods either for diagnostic purposes via single-photon emission computerized tomography (SPECT) imaging or therapy (Matichard et al., 2004). Melanocytes express MC1R highly in the majority (>80%) of both primary and metastatic melanoma cell lines (Salazar-Onfray et al., 2002; Seenivasan et al., 2015). However, MC1R has been mainly studied as a prognostic risk factor for melanoma skin cancer, indicating it could be deployed for the detection of high-risk groups and prevention measures (Matichard et al., 2004).

4.1.2. Cell regulative and tumour-promoting proteins

Cell regulative and tumour-promoting factors are valuable for developing diagnostic biosensors and reducing the frequency of false positive diagnoses. They hold the potential to be measured in blood or tissue samples using biosensing techniques, enabling monitoring of disease progression, and targeted therapies.

The microphthalmia-associated transcription factor (MITF) controls the development and expression of melanocytes and melanogenesis enzyme genes, but extracellular acidification during carcinogenesis results in its reduced expression (The Human Protein Atlas, 2022b). The factor is present intracellularly and has not been detected in other biological fluids, thus limiting its detection via immunohistochemical assays, without offering tissue specificity. Similarly, the MAGE-I subgroup is being overexpressed in breast, ovary, lung, testis and bladder cancer. They are known to promote tumour cell viability and inhibit cell

Table 1An outline of melanoma skin cancer biomarkers with clinically relevant characteristics.¹

Biomarker	Function	Sensitivity primary melanoma	Sensitivity metastatic melanoma	Diagnostic accuracy	Biological matrix	Melanoma associated serum levels	Normal serum levels	Ref.
PMEL17	Eumelanin polymerization	72–100%	58–95%	91–100%	Intracellular blood	NA	NA	(The Human Protein Atlas, 2022c; Weinstein et al., 2014)
Melan-A/MART-1	Expression and stability of PMEL	83–100%	71–88%	81–98%	Intracellular Extracellular matrix	NA	NA	Weinstein et al. (2014)
MC1R	Eumelanin production	NA	60%	NA	Intracellular Extracellular matrix	NA	NA	(Raposinho et al., 2010; Tagliabue et al., 2018)
MITF	Melanocyte development	100%	77–100%	87–100%	Intracellular	NA	NA	(The Human Protein Atlas, 2022b; Weinstein et al., 2014)
MIA	Facilitates cell metastasis	NA	95.5%	86.4%	Intracellular Serum	0.74–1.45 µg/L	0.45–0.78 µg/L	Li et al. (2021)
VEGF	Angiogenesis Cellular permeability	72–100%	57–100%	78%	Intracellular ISF Serum	0.035–0.414 µg/L	0.01–0.035 µg/L	(May et al., 2005; Redondo et al., 2000)
Tyrosinase	Synthesis of melanin	90–100%	63–93%	97–100%	Intracellular ISF Serum	0.066–0.636 U/L	0.006–0.06 U/L	(Merimsky et al., 1999; Sonesson et al., 1995; Weinstein et al., 2014)
S100B	Cell growth, motility, and differentiation	89–100%	86–100%	70–79%	Intracellular Plasma Serum	0.2–11 µg/L	<0.15–0.2 µg/L	(Barak et al., 2015; Gehring et al., 1998; Undén et al., 2005; Weinstein et al., 2014)
LDH	Converts pyruvate to lactate	NA	NA	NA	Intracellular ISF Serum	300–3000 U/L	140–280 U/L	(Desai et al., 2023; Zhang et al., 2021)

apoptosis, thus providing tumours with a growth advantage (Lian et al., 2018).

The melanoma inhibitory activity protein (MIA) was found to be highly expressed and exocytosed in malignant melanocytes (Riechers and Bosserhoff, 2014) and engage in the metastasis of melanoma skin cancer via augmented cell migration and immunosuppression (Riechers and Bosserhoff, 2014). A clinical study showed that MIA levels in serum were significantly higher in III-IV stage patients than I-II stage patients and healthy donors. Studies revealed that in the cases where MIA serum levels surpassed 914.7 pg/mL disease-free survival was predicted with 86.4% specificity and 95.5% sensitivity (Li et al., 2021), rendering it a prognostic marker for high-risk populations.

CEACAM1 is a transmembrane protein associated with the deterioration of metastatic melanoma due to its ability to enhance tumour cell invasiveness presenting significantly increased serum levels upon monitoring active patients (Draberova et al., 2000; Markel et al., 2010). A direct relationship was observed between the levels of CEACAM1 and LDH levels in high-risk metastatic patients, both being independently negatively correlated with survival suggesting that CEACAM1 has a systemic role in melanoma (Markel et al., 2010).

Garcia et al. discovered that the inner nuclear membrane protein LAP1 is overexpressed in primary migrating and metastatic melanoma cells making them more adaptable to microenvironment limitations during migration and contributing to tumour belligerence (Jung-Garcia et al., 2023). Furthermore, LAP1 expression in the tumour-invasive front was linked to shorter disease-free survival and poor prognosis.

Caveolin-1 (cav-1) is a cell membrane and exosomes protein, involved in various cellular processes thus targeting it can be a therapeutic strategy for treating melanoma (Diaz et al., 2020; Friedel et al., 2023). In melanoma cells, the expression of cav-1 is often

downregulated, which leads to increased cell proliferation and apoptosis. Cav1 levels in melanoma patients' blood are significantly higher than in healthy individuals providing potential diagnostic sensitivity based on the detection of cav1-positive (cav-1+) exosomes (68%) instead of other melanoma-related housekeeping proteins like CD63 (43%) (Logozzi et al., 2009).

The vascular endothelial growth factor (VEGF) has been studied for its role in the angiogenesis of malignant melanoma tumours (Redondo et al., 2000). As a mitogen promotes the formation of new blood vessels and increases the permeability of EC monolayers, thus the permeability of macromolecules and nutrients to the main tumour body (May et al., 2005). However, high blood VEGF is associated with renal, liver, endometrial, urothelial and cervical cancer, thus it is not melanoma-specific.

4.1.3. Tyrosinase-related proteins

Tyrosinase (TYR) is an ISF-detected enzyme that catalyzes the conversion of the amino acid tyrosine into dopaquinone which is subsequently converted into melanin and potentially induces tumour regression (Ghanem and Fabrice, 2011; Merimsky et al., 1999). The overexpression and hyperaccumulation render it a melanoma biomarker while being directly correlated to the level of malignancy. Monitoring the dynamic change of tyrosinase concentration could be a predictive factor for the progression of the disease (Ren et al., 2022).

The RT-PCR ("Reverse Transcriptase Polymerase Chain Reaction") method has been used to detect tyrosinase mRNA and produced very accurate results (Eftekhari et al., 2019). However, studies for tyrosinase mRNA in circulating blood have produced inconsistent results, which could be attributed to the temporary presence of melanoma cells in the bloodstream or the lack of established standards (Eftekhari et al., 2019).

The transmembrane glycoprotein TYRP1 is also involved in melanin synthesis as a component and transport factor of melanosomes, regulating TYR activity, and inhibiting melanocytic cell death (Bolander et al., 2008; Ghanem and Fabrice, 2011). TYRP-1 is overexpressed in the majority of metastatic melanoma tissues and is associated with tumour stage but not with overall or disease-free survival (Bolander et al., 2008; Escors, 2014).

¹ PMEL17 (premelanosome protein 17), Melan-A/MART-1 (melanocytic membrane protein/melanoma antigen recognized by T-cells-1), MC1R (melanocortin-1 receptor), MITF (microphthalmia-associated transcription factor), MIA (melanoma inhibitory activity protein), VEGF (vascular endothelial growth factor), LDH (lactate dehydrogenase).

4.1.4. S-100 family proteins

S-100 family proteins are extracellularly secreted in melanocytes (Jing et al., 2013) but due to their involvement in various physiological cellular processes during histopathology staining they are identified concurrently with other markers (Heizmann, 2019; Weinstein et al., 2014). The binding protein S100B has been detected in blood (The Human Protein Atlas, 2022d) and elevated levels of S100B in the serum of stage III patients are a robust predictor of melanoma-specific survival. Monitoring S100B levels has proven beneficial in assessing the response to immunochemotherapy treatments like dabrafenib and vemurafenib. It is recommended to monitor the serum levels of S100B for a period of 10 years in advanced-stage patients when the levels surpass 0.13 µg/L (Bouwhuis et al., 2011) since levels above 0.6 µg/L can increase the relative death rate by 5-fold (Eftekhari et al., 2019). cDNA analysis of patients with advanced disease states revealed increased S100A8 and S100A9 gene expression in metastases compared to primary melanomas and serum levels greater than 5.5 mg/L were linked to poor overall survival (Wagner et al., 2019).

4.2. Genetic mutations and nucleic acids

The BRAF mutation is an oncogenic initiator in melanoma; upregulates the mitogen-activated protein kinase (MAPK) pathway while detected in 66% of genetic alteration cases in melanoma cells (Rosenkranz et al., 2013; Wuethrich et al., 2021). BRAF controls among others processes cell proliferation, migration, and survival (Huber et al., 2013). The constitutive stimulation of BRAF/MAPK signalling maintained by the BRAFV^{600E} kinase mutant is linked to the increase of glycolysis which is the primary energy source for melanoma skin cancer (Avagliano et al., 2020).

Recently, microRNAs (miRNAs) were identified as post-transcription regulators of gene expression, carcinogenesis, and disease progression. Some miRNAs, like miR-214 and miR-203, are pleiotropic thus dysregulating gene expression and facilitating tumour suppression in many tumours (Gerloff et al., 2020; Neagu et al., 2020). On the contrary, miR-21 and miR-221, which are regulated by the MITF, are specific for melanoma and squamous cell carcinoma (Gerloff et al., 2020; Neagu et al., 2020). miRNAs have been extracted from exosomes that carry specific cell surface markers, but their clinical and diagnostic for melanoma should be further certified (Choi et al., 2022; Eftekhari et al., 2019).

4.3. Other molecular and microenvironmental factors

Microenvironmental changes in pre-malignant lesions impact melanoma tumour formation (Boussadia et al., 2018; Sahu et al., 2019). The skin's normal inner layers are slightly alkaline ($\text{pH } 7.3 \pm 0.1$) (Gunathilake et al., 2009), however, tumour development acidifies the microenvironment due to increased glycolysis and lactate accumulation, resulting in pH decreases as low as 6.4 (Boussadia et al., 2018; Vaupel et al., 1989). The Na^+/H^+ exchanger, regulated by the prevalent melanoma mutation BRAFV600E, induces pH dysregulation and metastatic spread (Koch and Schwab, 2019). miR-211, a potential target for hypoxia-induced cell death, is frequently lost during melanoma development (Dratkiewicz et al., 2021) and activated fibroblasts, a significant portion of the tumour mass (80%), secrete elevated VEGFA under hypoxia, influencing angiogenesis (Dratkiewicz et al., 2021). Lactic acid is consistently found in interstitial fluid (ISF) samples (Samant et al., 2020) and elevated lactate leads to increased serum LDH (Dratkiewicz et al., 2021; Keung and Gershenwald, 2018; Palmer et al., 2011). Notably, serum LDH levels gauge the effectiveness of therapeutic agents like nivolumab, pembrolizumab, and ipilimumab.

5. Biosensing technologies for skin cancer diagnosis

With increasing skin cancer rates and the limitations of biopsies,

researchers are striving for biosensing breakthroughs that could be integrated into portable POC devices, enhancing accessibility, eliminating inter-clinician variability, providing highly accurate results and mitigating the consequences of late skin cancer diagnosis.

5.1. Proteins and enzymes towards melanoma detection

5.1.1. Detection of malignant melanoma cells

Sensor-based imaging and immunosensing have advanced to detect melanoma cells with high specificity and sensitivity, enhancing melanoma diagnosis accuracy, especially in biopsies and surgery when positive margins indicate the risk of recurrence.

A recently developed infrared (IR) sensor examines skin biopsy sections to identify malignant melanoma cells by recording the 3330–3570 nm absorption spectra using a micron-scale light spot and a monochromator while deploying a versatile computational environment for controlled data acquisition, processing, and storage (Fioravanti et al., 2016). The detection principle owes to the fact that cancerous areas demonstrate different spectral forms with significantly higher methylene (H–C–H) stretching ratios compared to normal tissues (Fig. 5a). The presented label-free IR sensor could be a supportive tool during the histopathological assays thus decreasing the risk of misdiagnosis. Due to enhanced deep penetration and decreased nonspecific fluorescence, near infrared-emitting fluorophores (NIR) have demonstrated higher tumour-to-background ratios, rendering NIR-based imaging techniques a powerful solution for cancer diagnosis and resection (Keereweer et al., 2012). Zambito et al. created a cell-based diagnostic sensor that uses dual-optical imaging to detect subcutaneous metastatic melanoma cells. For dual-colour bioluminescence imaging *in vivo*, tumour-associated macrophages (TAMs), which accumulate in hypoxic areas and infiltrate melanoma tissues, were engineered to express a green luciferase and an NIR fluorescent dye, while melanoma cells were engineered to express an NIR red luciferase (Fig. 5b) (Zambito et al., 2022). An IVIS spectrum imager captured real-time *in vivo* images and generated a signal intensity map of the bioluminescent and fluorescent signals. The researchers demonstrated that engineered macrophages at a concentration of 10 million could detect and significantly accumulate in subcutaneous metastatic melanoma in a clinically relevant murine model with subcutaneously engrafted cells.

Increased interest exists in developing real-time techniques for improving intraoperative micromelanoma detection, especially with positive margins indicating incomplete tumour cell removal. Day et al. identified the optimal FDA-approved fluorescently labelled antibody for imaging in a preclinical murine ear model mimicking metastatic melanoma, laying the groundwork for an intraoperative melanoma recognition sensor (Day et al., 2013). Researchers leveraged NIR fluorescence for studying bevacizumab, panitumumab, and tocilizumab antibodies targeting VEGF, EGFR, and IL-6R. All exhibited superior tumour-to-background ratios over non-specific IgG antibodies, with bevacizumab and panitumumab also aiding residual disease detection and improving tumour resections. Despite their effectiveness in distinguishing tumours and overexpressed EGFR, VEGF, and IL-6R in Western blot analysis, these antibodies lack melanoma specificity, necessitating further scope development.

Recent breakthroughs in identifying and quantifying CTCs and isolating tumour vesicles in patients' blood have revolutionized the potential of liquid biopsy for cancer diagnosis, prognosis, and management, including melanoma. To this end, a novel electrochemical immunosensing strategy has been developed using polyaniline (PANI) nanofibers functionalized with anti-MC1R antibody and a screen-printed electrode (SPE) platform, aiming to detect melanoma cells by targeting the MC1R cell surface protein (Prathap et al., 2018). The PANI nanofibers are chosen for their unique electrical properties, stability, and ability to effectively bind and immobilize biomolecules. The experimental parameters of the immunosensor were optimized to achieve a limit of quantification of 1 cell/mL and a relatively wide linear

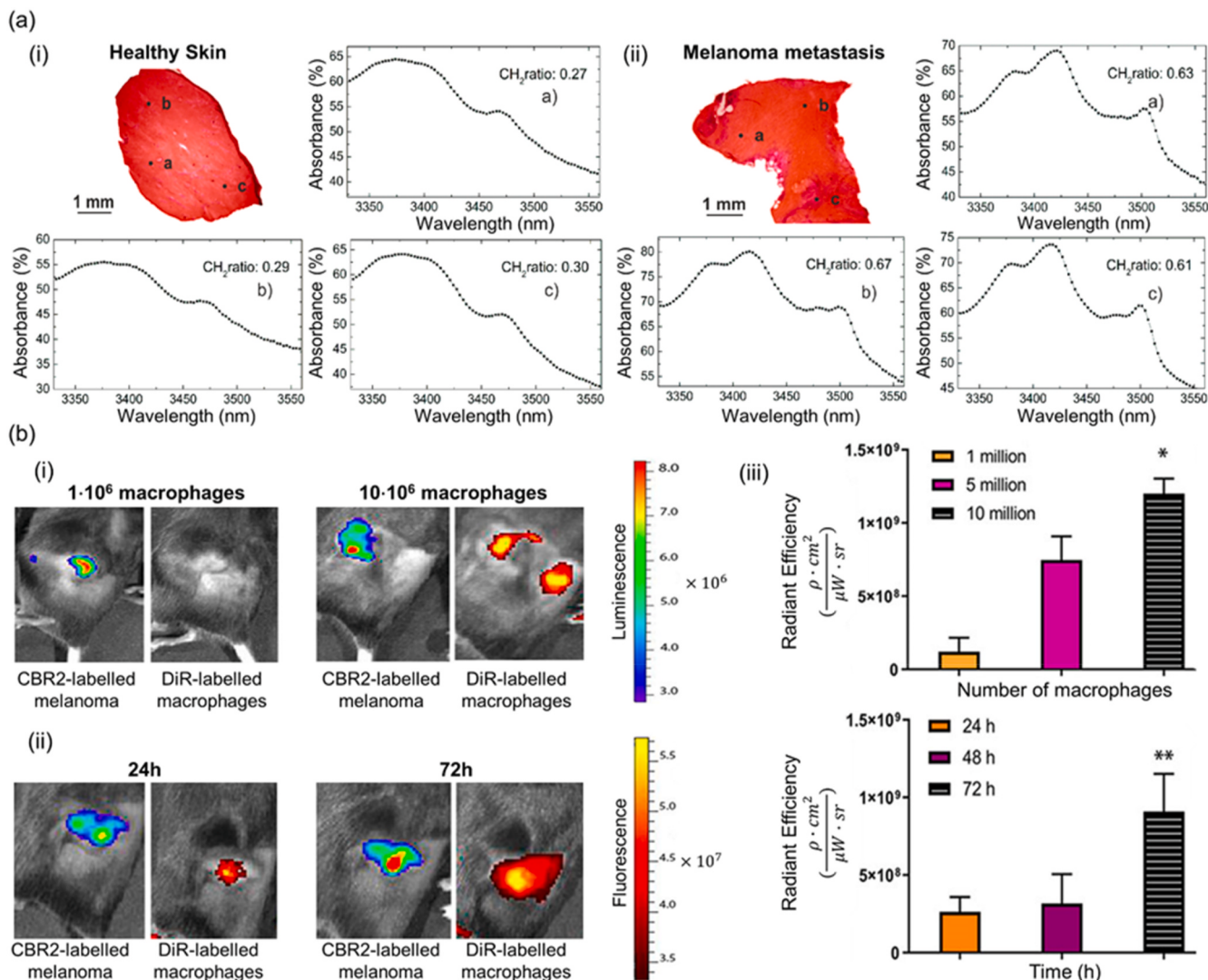


Fig. 5. Infrared biosensors for the detection of metastatic melanoma cells: (a) Haematoxylin/eosin-stained pictures of (i) healthy and (ii) metastatic melanoma tissue investigated by the IR sensor featuring the difference in CH₂ stretch ratio values as obtained from three skin biopsy samples (Fioravanti et al., (2016); Copyright © 2016 Fioravanti et al. (Reproduced under terms of the CC-BY license). (b) Dual-colour bioluminescence and fluorescence *in vivo* sensing of melanoma with tumour-associated macrophages: (i) the signal intensity maps and the quantified radiant efficiencies of 1, 5 and 10 millions of subcutaneously injected DiR-labelled macrophages juxtaposed with CBR2-labelled xenografted melanoma cells (ii) fluorescence values and the respective radiant efficiencies of 10 million DiR-labelled injected macrophages compared to CBR2-labelled xenografted melanoma cells post-injection (Zambito et al., (2022); Copyright © 2022 Zambito, Mishra, Schlieke and Mezzanotte (Reproduced under terms of the CC-BY license).

range from 15 to 7000 cells/5 mL tested in a suitable solution, given the high surface area of the nanofibers. Targeting melanoma cells was very specific as the sensor did not respond to normal human embryonic kidney cells. Also, a theragnostic hybrid graphene oxide-based assay that can selectively detect G361 melanoma CTCs in blood samples has been developed (Viraka Nellore et al., 2014). Detecting CTCs in blood demands exceptional sensitivity hence the G361-specific AGE-aptamer was utilized, conjugated with indocyanine green (ICG) on magnetic nanoparticles. These were attached to a hybrid graphene oxide platform enabling multi-colour luminescence. The malignant cells that bonded to the aptamer-graphene oxide detection system were separated by the blood sample with a bar magnet at 97% efficiency. The distinction of the malignant melanoma cells present in the blood sample was achieved by detecting the melanoma inhibitor of apoptosis protein (ML-IAP) via ELISA. The ICG-bound magnetic nanoparticles achieved 99% cell death efficiency functioning as combinational photodynamic and photo-thermal therapeutic agents (Viraka Nellore et al., 2014). The developed theragnostic tool could be very beneficial for POC applications, once

properly validated in clinically relevant samples, and concentrations.

Seenivasan et al. proposed a portable approach of an electrochemical immunosensor which in the future if coupled with a microfluidic “lab-on-a-chip” platform could detect CTCs in blood samples (Seenivasan et al., 2015). The proposed system is highly selective as it relies on the affinity between the protein MC1R and the anti-MC1R antibody (MC1R-Ab) which was immobilized via amino-functionalized silica nanoparticles (n-SiNPs) on polypyrrole (PPy) nanocomposites (Fig. 6a). To detect the alteration of the produced electrochemical signal the researchers studied the anodic oxidation current, using ferricyanide as the redox mediator. The antigen–antibody interaction decreases the voltammetric peak by hindering the electron transfer reaction of the redox mediator and the sensor surface. Although an adequate quantification limit of 20 cells/mL and a linear performance was achieved, the performance of the immunosensor integrated with a microfluidic system should be further investigated to function as a clinical diagnostic tool. Thus, Prathap et al. developed and optimized an immuno-electrochemical biosensor integrated into a microfluidic

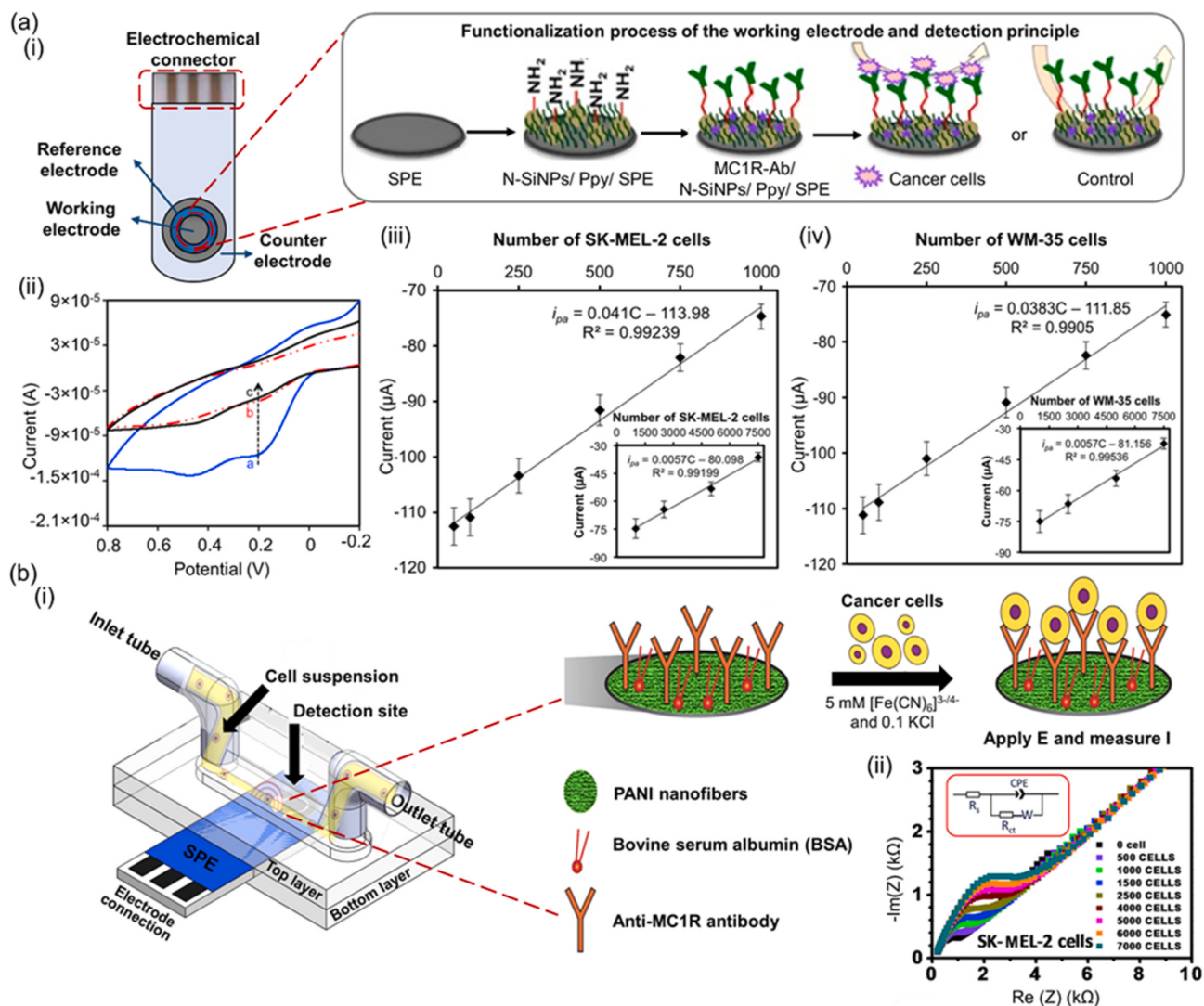


Fig. 6. Electrochemical immunosensors that are founded on the binding affinity of the same antigen-antibody system (MC1R-anti-MC1R): (a) (i) schematic of the proposed biosensing device which relies on the affinity of MC1R-ab-MC1R and description of the antigen immobilization process on the amino-functionalized n-SiNPs on PPy nanocomposites on the surface of the SPE electrode, (ii) CV responses of the immunosensor generated by the detection of CTS generates an electrochemical signal with the curves corresponding to (a) the control, the presence of (b) 7500 SK-MEL-2 cells/2.5 mL and (c) 7500 WM-35 cells/2.5 mL, (iii) the decreases in anodic peak current at +0.195 V in the presence of SK-MEL-2 melanoma cells ranging from 0 to 7500 cells/2.5 mL, (iv) the decreases in anodic peak current, respectively, in the presence of WM-35 melanoma cells ranging from 0 to 7500 cells/2.5 mL [Seenivasan et al., \(2015\)](#); Copyright © 2015 Elsevier B.V. (b) (i) schematic of the nanofiber-antibody-based microfluidic device with distinct layers (SPE electrode, functionalized detection site and circulating cell suspension), (ii) the immobilization of the anti-MC1R on the PANI nanofibers as the immunoassay for cell detection leads to the acquisition of a Nyquist plot for the MC1R-Ab-PANI/SPE electrode for various concentrations of SK-MEL-2 melanoma cells. [Anu Prathap et al., \(2019\)](#); Copyright © 2019 Elsevier B.V.

system to detect MC1R in circulating melanoma cells ([Anu Prathap et al., 2019](#)). The same antigen-antibody system (MC1R-anti-MC1R) was employed, nonetheless, this time the anti-MC1R antibody was covalently immobilized to polyaniline nanofibers (PANI)-modified working electrode surface on a screen-printed electrode (SPE), which was incorporated in a PDMS microfluidic channel for cell sample circulation ([Fig. 6b](#)). A significantly low limit of quantification (1 cell/mL) was accomplished in a solution containing peripheral blood mononuclear cells, while the signal was log-linear from 1 to 900 melanoma cells/mL ([Anu Prathap et al., 2019](#)). Electrochemical impedance spectroscopy (EIS) results highlight this sensor as a unique, promising candidate for metastatic cancer diagnosis due to its remarkably low melanoma CTC detection limit, all within a portable device.

5.1.2. Detection of cell signalling proteins

Detecting melanoma skin cancer via cell signalling proteins offers early, accurate diagnosis compared to traditional methods. These

proteins impact cell adhesion, migration, cell cycle regulation, and intracellular trafficking, alterations to which may arise before visible changes manifest on the skin.

Overcoming the reportedly low concentration of CD146, a melanoma-associated antigen, a novel immunosensor was created using aminated graphene (GS-NH₂), mesoporous nano-Co₃O₄ sheets, and gold nanoparticles (AuNP/Co₃O₄) ([Ren et al., 2014](#)). The AuNP/Co₃O₄ in the immunosensor increased the contact surface area thus the electron transfer between the antibody and the AuNPs attached to the Co₃O₄, while the mesoporous Co₃O₄ nanosheet facilitated the capture of more biomolecules, thereby enhancing sensitivity via dual amplification. The recognition of CD146 was achieved with amperometry and EIS, demonstrating a broad linear range (0.01–15 ng/mL), with a low detection limit (3.4 pg/mL). The system was also evaluated in human serum, yielding satisfactory results and providing a promising approach for use in clinical diagnostics.

C. Prével et al. developed a fluorescent peptide biosensor to quantify

the activity of CDK4 (cyclin-dependent kinase 4), which is activated by binding to the specific protein cyclin D and is known to be dysregulated in 90% of melanomas (Prevel et al., 2016). Hyperactivation of CDK4, amplification of Cyclin D, or downregulation of the tumour suppressor protein p16^{INK4a}, is linked to elevated risk of developing cutaneous melanoma. The peptide biosensor incorporates a sequence of fluorescently labelled amino acids that is phosphorylated by CDK4/Cyclin D with specificity. Fluorescent activity was recorded in cell extracts, skin biopsies, and melanoma xenografts offering an alternative to immunological biorecognition.

5.1.3. Tyrosinase detection with signal enhancing modalities

The development of biosensors that can sensitively monitor the levels of tyrosinase (TYR) has attracted the interest of many scientists. To address this issue Chenyue Zhan et al. created a fluorescent imaging probe (namely NBR-AP), to detect primary and metastatic melanoma *in vitro* (B16-F10 cells) and *in vivo* (rodent model) (Fig. 7b) (Zhan et al., 2018). The probe consists of a hydroxyphenyl-urea group (enzyme substrate) combined with a fluorescent dye phenoxazine derivative, which acts as a signal reporter activating the probe in the presence of tyrosinase through an oxidation process, which sequentially leads to the breakdown of the urea linkage and emission of fluorescence. The NBR-AP probe showed a strong direct correlation between fluorescence intensity and tyrosinase concentration, ranging from 0 to 200 U/mL (Zhan et al., 2018). During *in vivo* studies, per the fluorescence intensity,

the levels of tyrosinase in the cancerous areas were determined to be much higher than in unaffected tissues. Kumar et al. studied the specificity of two turn-on-off fluorescent probes founded on naphthalimide derivatives with mono and dihydroxy phenol groups, as these groups have been shown to have a high affinity for tyrosinase (Kumar et al., 2020). They can detect elevated levels of tyrosinase, ranging from 5 U to 10 U, rapidly, with fluorescence reaching full quenching within 5 min. The probes are able to detect tyrosinase at nanomolar concentrations (2 nM) and can be used for live-cell fluorescence imaging as shown by *in vitro* studies.

Carbon quantum dots are attractive for biosensing applications, especially for cancer detection, due to their small size, strong fluorescence properties, biocompatibility, and ease of synthesis. Lujing Chai et al. worked on a highly selective biosensor for monitoring TYR activity based on biocompatible dopamine-functionalized carbon quantum dots (Dopa-CQDs) as fluorescence probes (Chai et al., 2015). The working principle of the assay relies on the catalytic oxidization of the dopamine molecules in Dopa-CQDs by tyrosinase, which leads to the formation of a dopaquinone derivative, resulting in an electron transfer between the CQDs and dopaquinone (Fig. 7c) (Chai et al., 2015). This process results in fluorescence quenching. The quantitative evaluation of tyrosinase activity corresponded to the fluorescence quenching efficiency. The assay was linear range from 23.2×10^{-3} to 793.5×10^{-3} U/mL with a detection limit of 7×10^{-3} U/mL. The results also showed that the Dopa-CQD system is biocompatible and can effectively detect changes in

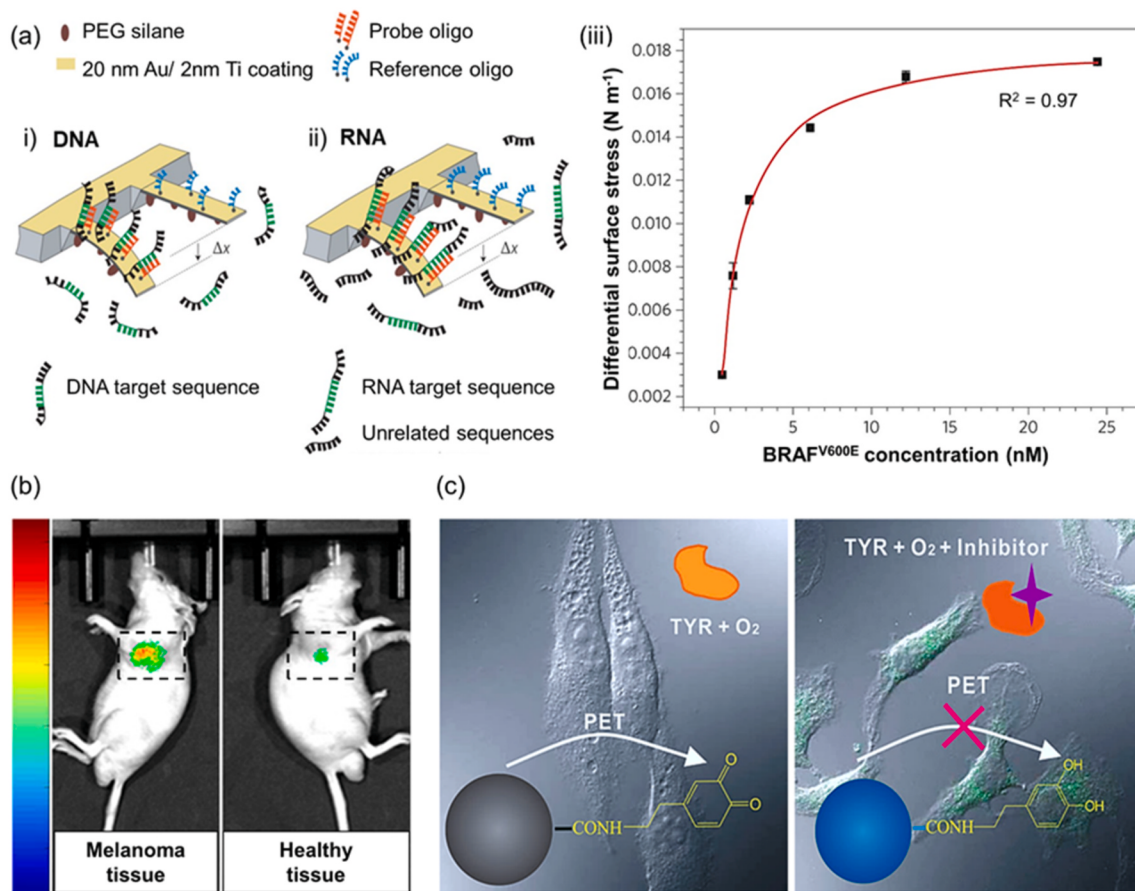


Fig. 7. Gene and enzyme-based applications for malignant melanoma detection: (a) A microcantilever-array-based sensor for detecting BRAF mutations in RNA from melanoma cells with a schematic of the working principle of the sensor (Huber et al., 2013) (i) the coating of the surface with PEG-silane (polyethylene-glycol-silane) averts non-specific adsorption and the array is coated with gold to enable thiol binding (iii) cantilevers are functionalized with a reference or probe oligonucleotides which detect complementary DNA or RNA sequences (iii) Successful hybridization results in cantilever bending. Copyright © 2013 Nature Publishing Group (b) A fluorescent probe for melanoma detection by targeting tyrosinase activity in injected melanoma cells (B16F10) juxtaposed with healthy cells (HeLa) in a mouse model (Zhan et al., (2018); Copyright © 2018 American Chemical Society. (c) Functionalized DOPA-CQDs for intracellular tyrosinase detection in melanoma cells through inhibition of the photoinduced electron transfer (PET) (Chai et al., (2015); Copyright © 2015 American Chemical Society.

tyrosinase levels within melanoma cells. Working under the same principle, J.J. Hu et al. expanded the linear response in the range of 0.711–2.925 U/mL with a detection limit of 17.7×10^{-3} U/mL (Hu et al., 2017).

Except for carbon quantum dots, gold nanoclusters have been implemented for tyrosinase sensing. X. Yang et al. synthesized a novel fluorescent probe for tyrosinase detection consisting of gold nanoclusters stabilized with L-tyrosine (AuNCs-Tyr) (Yang et al., 2014). The affinity between L-tyrosine and tyrosine was due to the stabilizing effect of L-tyrosine on the gold nanoclusters and the specific interaction between tyrosine and tyrosinase during catalytic reactions. The determination of tyrosinase activity was based on the aggregation of AuNCs@Tyr on the active sites of the enzyme, leading to the quenching of their fluorescence. Tyrosinase activity was determined linearly from 0.5 to 200 U/mL with a sensitivity of 0.08 U/mL, without yet having been tested in clinically relevant conditions. Researchers developed a ratiometric fluorescent technique using glutathione-protected AuNCs to measure tyrosinase concentration and catalysed dopamine in a linear range of 0.006–3.6 U/mL and 1.0 nM to 1.0 mM, respectively (Teng et al., 2015). Another approach for determining tyrosinase presence based on dopamine-modified gold-silver nanoclusters (Dopa-Au/Ag NCs) bioconjugated with a fluorophore agent was introduced by H. Ao et al. (2016). Upon the oxidization of dopamine in the presence of tyrosinase, electron transfer occurs between the NCs and

o-dopaaquinone, leading to fluorescence quenching (Stoitchkov et al., 2002). The acquired fluorescence signal offered a quantitative evaluation of tyrosinase levels from 0.045 to 0.3195 U/mL with a detection limit of 0.0135 U/mL (Ao et al., 2016).

Diagnosis of malignant melanoma has also been studied in correlation to the DOPA/Tyrosinase ratio, an indicator supported by clinical studies (Stoitchkov et al., 2002). Based on this data, S.B. Revin and S.A. John developed an electrochemical marker on glassy carbon able to investigate the DOPA/Ty ratio in serum samples with cyclic voltammetry by deploying a pAMTA electrode which could successfully prevent biofouling (Revini and John, 2013). The signal increased linearly as DOPA and tyrosinase levels augmented in the range of 10^{-8} – 10^{-4} M and 5×10^{-8} – 10^{-4} M, respectively, with detection limit of tyrosinase corresponding to 1.9×10^{-10} M.

As recent biosensing technologies have shifted towards minimally invasive detection methods, Ciui et al. developed a minimally invasive microneedle biosensor for decentralized cutaneous melanoma screening, using TYR detection (Fig. 8a and b) (Ciui et al., 2018). Hollow microneedles, produced via 3D printing, were polished with graphite-enriched carbon paste and functionalized with the catechol (CAT) substrate which was constrained in a conductive hydrophilic gel serving as an electrochemical cell (Fig. 8c and d). The base of the microneedles was connected to a transduction system of flexible electronics. This biosensor, based on current signals generated by

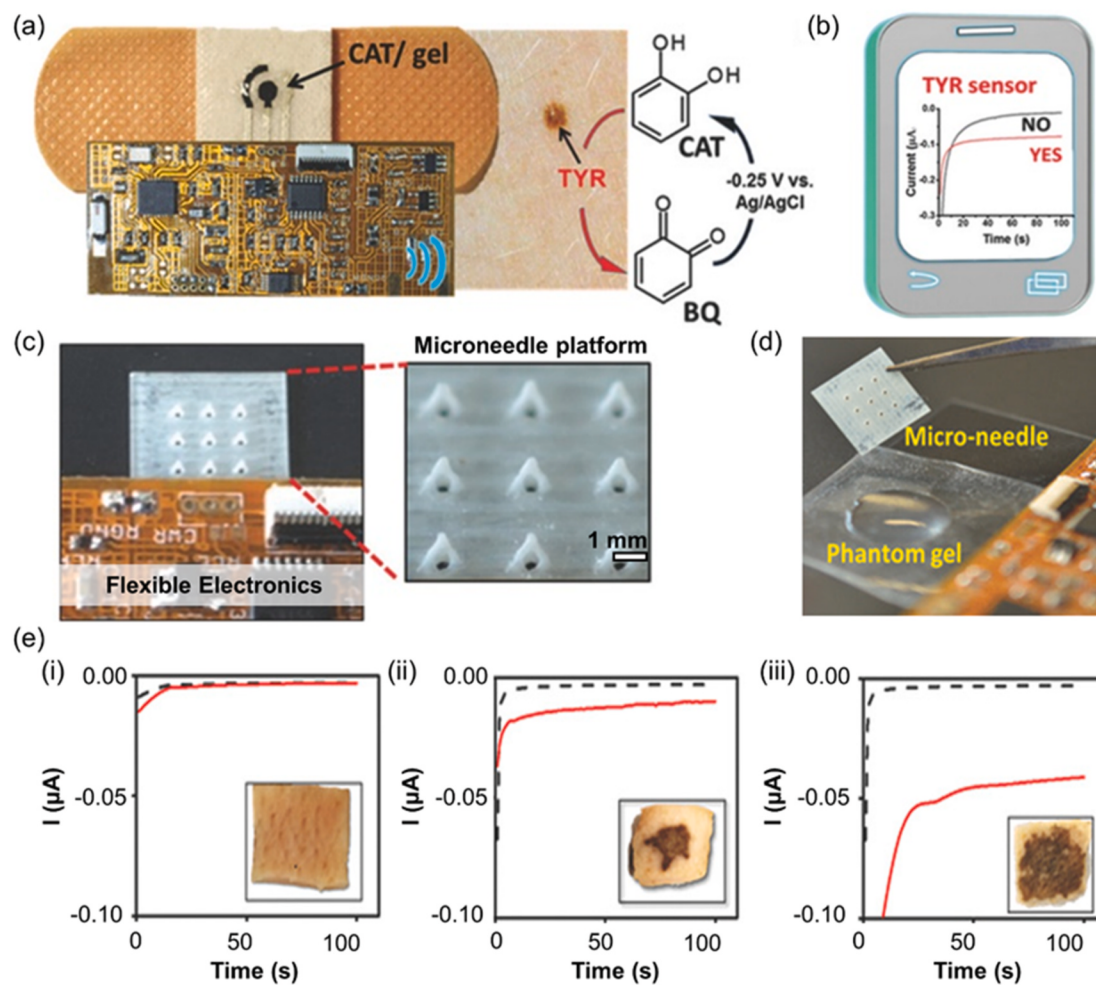


Fig. 8. Bandage sensor for cutaneous TYR detection: (a) TYR sensing on a bandage with flexible electronics. (b) Wireless data transfer. (c) Microneedle's integration with the electrochemical sensor (needle hole diameter: 425 μm). (d) Experimental set-up for the sensor's validation in a representative skin gel model (phantom gel) artificially doped with TYR, using the built-in electronic board. (e) Amperometric ex vivo validation of the microneedle-based sensor in porcine skin model treated and incubated with 0 (i), 0.5 (ii) and 2.5 mg/mL (iii) TYR for 24 h; the notable change in skin colour was due to the interaction of dermal cells with the enzyme. Ciui et al., (2018); Copyright © 2018 WILEY-VCH.

TYR-induced CAT conversion to benzoquinone, exhibited promising sensitivity (slope: $4.6 \mu\text{A}/\text{mg} \cdot \text{mL}_{\text{TYR}}$), for TYR detection (Fig. 8e). Efforts could focus on clinical investigations to validate the efficacy of the sensor in different stages of skin cancer.

Furthermore, a high-performance field-effect transistor-based biosensor (bio-FET) has been successfully developed by self-assembling nanostructured tetrapeptide tryptophan–valine–phenylalanine–tyrosine (WVFY) on n-type metal oxide transistors for tyrosinase detection (Fig. 9a) (Ren et al., 2022). The WVFY peptide has been used due to its ability to self-assemble onto the surface and serve as a recognition element for tyrosinase, which induces the conversion of the phenolic hydroxyl groups of the peptide to o-benzoquinone and a detectable potentiometric signal is generated. Ren et al. designed flexible wearable polyimide (PI)-based substrates to detect this signal with favourable mechanical properties for conformal skin attachment (Fig. 9b and c). The peptide-modified sensor presented a very low detection limit of 1.9 fM with a wide detection range of $10 \text{ fM}-1\text{nM}$, thus holding great potential for tyrosinase detection and melanoma screening while laying the groundwork for wearable cancer screening bio-FET technologies (Fig. 9d). This technology could also be employed for large-scale research studies aiming to quantify tyrosinase levels in distinct cancer stages, however, the accuracy of this approach should be further validated. Also, Wang et al. developed a novel SERS sensor, by assembling AuNPs and p-thiol catechol on an indium tin oxide electrode as the SERS substrate, for detecting TYR due to the spectral variation triggered by the catalysis of p-thiol catechol to p-thioquinone (Wang et al., 2019). The sensor exhibited rapid response ($<1\text{min}$), high selectivity, and low detection limit (0.07 U/mL). This portable device is a breakthrough of high importance as it can provide high sensitivity and specificity by allowing the real-time detection of molecular vibrations unique

to TYR, but it should be evaluated in complex biological samples.

5.1.4. Detection methods for S100B

Multiple methods have been developed towards S100B, including electrochemical approaches and the functionalization of microneedles with an anti-human S100B detection antibody. X. Wang et al. developed an electrochemical assay for the detection of S100B in human blood samples utilizing the 1:2 binding ratio between the melanoma biomarker and a peptide that recognises with specificity S100B (Wang et al., 2014). A specific capture peptide enabled the biorecognition of S100B, while a signal peptide, that bonded with the protein due to the Gly-His-Lys modification, concurrently facilitated signal amplification and offered higher sensitivity. From studies performed in S100B doped samples under square wave voltammetry, a very low LOD (0.1 nM) and a positive correlation within the range of $0.1-25.6 \text{ nM}$ were achieved, while almost 100% marker recovery was accomplished in serum samples. The recognition of S100B was also studied by researchers who developed an electrochemical immunosensor using a chitosan/reduced graphene oxide (CS-rGO) nanocomposite (Zhang et al., 2022a). The sensor worked by measuring the decreased current signal of electrochemical probes, resulting from the antigen-antibody complex formation at the electrode interface which increased steric hindrance. The nanocomposite offered excellent conductivity and biocompatibility, resulting in augmented stability, selectivity, sensitivity, and a wide range of 10 fg/mL to $1 \text{ }\mu\text{g/L}$, with a low LOD of 1.9 pg/mL , measured with differential pulse voltammetry. The sensor was tested on artificially protein-doped real human serum samples, demonstrating good reliability with a recovery of S100B ranging from 97.4% to 105%. Totti et al. also extracted and detected S100B *in situ* on a 3D tissue-engineered

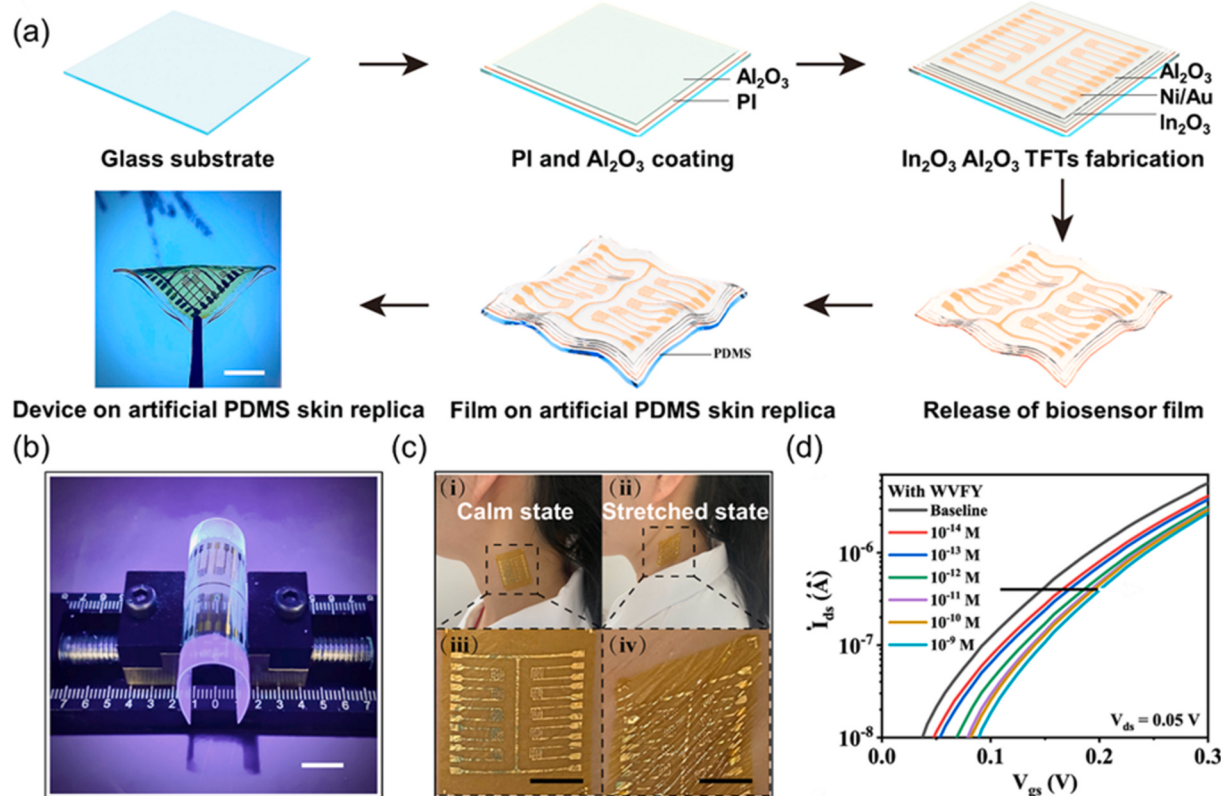


Fig. 9. Flexible FET for tyrosinase detection: (a) The fabrication process of the flexible bio-FET-based sensor; the bio-FET array was created by coating a glass substrate with a PI film, an Al₂O₃ buffer layer, and an In₂O₃ channel layer with interdigitated source/drain electrodes of Ni/Au, followed by spin-coating of an Al₂O₃ precursor, delamination of the bio-FET array from the glass substrate, and conformal attachment to the skin resembling PDMS substrate. (b) The device under bending deformation, scale bar: 1 cm. (c) Images of the Al₂O₃/In₂O₃ bio-FET arrays attached to human neck skin in (i) calm and (ii) stretched states, (iii-iv) magnified view, scale bars: 50 mm. (d) Transfer curves of the WVFY-based (tryptophan–valine–phenylalanine–tyrosine)device measured in PBS dosed with various concentrations of tyrosinase: 0, 10^{-14} M , 10^{-13} M , 10^{-12} M , 10^{-11} M , 10^{-10} M , and 10^{-9} M . (Ren et al., 2022; Copyright © 2021 Ren et al.)

disease model using microneedles functionalized with an anti-human S100B detection antibody (Totti et al., 2019). A novel blotting method was used to identify the captured S100B and subsequently the obtained amount of S100B was calculated by juxtaposing the blotting and coating pattern. Future research should enhance the reliability and efficiency of these clinical detection methods.

5.2. Nucleic acids towards melanoma detection

A group of new nucleotide phosphoramidites synthesized and incorporated in DNA probes with pyrene-modified fluorescent phosphates was developed by P. Li et al., (2016). These probes exhibit decreased fluorescence due to the quenching effect of the nucleobases but emit a strong signal when a perfectly matched duplex is formatted. They were used as “on-off” fluorescence sensors for detecting single nucleotide polymorphisms (SNPs) and successfully detected a specific BRAF mutation in human melanoma during PCR applications via fluorescence spectrophotometry. With a more advanced approach, Wuethrich et al. created a microcantilever-array-based method for directly detecting BRAF mutations in total RNA from melanoma cells without resorting to real-time polymerase methods (Fig. 7a) (Huber et al., 2013). By deploying an oligonucleotide probe that consists of a complementary sequence specific to BRAF^{V600E}, the assay can detect the mutation requiring only 20 ng/ml of RNA, thus advocating its suitability for clinical applications, while the surface stress generated upon detection is correlated to the concentration of the mutation (Huber et al., 2013). This methodology could facilitate and accelerate tumour identification, reducing treatment time. The parallel array format makes this cantilever method adaptable to other malignancies, offering comprehensive clinical prognosis alongside melanoma screening. Considering the diagnostic importance of detecting the BRAF gene mutations, scientists developed an integrated multimolecular sensor (IMMS) to identify the distinct mutation BRAF^{V600E} in circulating melanoma cells from liquid biopsy samples (Wuethrich et al., 2021). An electrochemical transducer is coupled with melanoma-specific cell capture and lysis mechanisms to allow the detection of BRAF^{V600E} simultaneously at DNA and protein levels. The differential pulse voltammetry-based detection method relies on antigen identification by the surface-immobilized anti-BRAF^{V600E} antibody with [Fe(CN)₆]⁴⁻ (Wuethrich et al., 2021). This device has been validated on plasma samples containing diagnostically relevant concentrations, hence it could pave the way for a new class of cancer biosensors for multimolecular analysis of liquid biopsies.

As evidence for the clinical utility of cell-free nucleic acids (cfNAAs) in bodily fluids has accumulated, technologies that can identify them have immense potential for individualized diagnosis and disease advancement. Specifically, the experimental data suggests that ISF contains comparable amounts of all RNA species, including miRs, previously discovered in the blood (Al Sulaiman et al., 2019). Sulaiman et al. developed a peptide-based hydrogel-coated microneedle patch to sample, isolate, and detect a DNA equivalent of miR-210 from skin interstitial fluid (ISF) with sequence-specificity. The microneedles were functionalized with custom-designed peptide nucleic acid (PNA) fluorescently labelled probes that were fixed to an alginate hydrogel matrix. The alginate hybrid PNA hydrogel allowed for rapid sampling and a significant fluid loading capacity of 6.5 µL within 2 min. With minimally invasive sampling of dermal ISF, the target DNA was hybridized with the PNA probe to a duplex whose fluorescence intensity was measured with a sensitivity of 6–500 nM, either on the patch or in a solution post-sampling. The importance of cell-free nucleic acids as informative biomarkers highlights the potential of automated and minimally invasive technologies for personalized diagnosis and continuous monitoring of disease progression in patients.

5.3. Olfactory detection of volatile organic compounds

Canine olfactory detection of human diseases, starting with a 1989

report of a dog detecting melanoma in its owner, has gained increased attention (Williams and Pembroke, 1989). However, recent research indicates limitations in practicality (Bauér et al., 2022; Willis et al., 2016). Addressing the challenges of canine-based melanoma detection, electronic noses (e-noses) are emerging as promising alternatives, mimicking canine olfactory capabilities. E-noses detect volatile organic compounds (VOCs) and have shown promise in oncology diagnostics, albeit influenced by environmental factors (Scheepers et al., 2022). D'Amico et al. developed a method for VOC detection in skin lesions, achieving 80% prediction accuracy using an array of seven quartz microbalance (QMB) chemical sensors (D'Amico et al., 2008). Their work showcased discernible gas chromatogram disparities in skin surface samples' headspace, collected from dermatology patients, distinguishing melanoma from nevus. The sensors gauged resonant frequency shifts proportional to gas-absorbed molecule mass, contributing to distinct patterns suitable for classification via pattern-recognition algorithms. Nevertheless, a comprehensive review of 208 studies from 1984 to 2020 revealed limited research on melanoma detection through e-noses, highlighting challenges and potential for improvement (Gouzerh et al., 2022).

5.4. Other biosensing approaches for detecting melanoma

VEGF has been also explored by May et al. by creating a cell-based biosensor for prompt diagnosis of metastatic melanoma in blood samples (May et al., 2005). The cellulose triacetate membrane of an ion-selective electrode, whose responsiveness increased proportionally to the VEGF content, was covered and incubated with a confluent monolayer of melanoma cells. The biosensor demonstrated a detection limit of 70 pg/mL equivalent to 210 M, indicating that it could for quantifying the levels of VEGF in blood samples from advanced cancer patients.

Based on the electrochemical signal generated by the interaction of the antigen MAGE-I and its corresponding antibody when immobilized on an indium tin oxide electrode (ITO), a novel low-cost immunosensor was created for the rapid identification of melanoma cancer (Gundogdu et al., 2017). By deploying electrochemical impedance spectroscopy (EIS), cyclic voltammetry (CV), and single frequency impedance (SFI) to investigate the antigen-antibody interactions, A. Gündogdu et al. managed to design an immunosensor that exhibits a low detection limit of 1.30 fg/mL as well as wide linear range from 4 to 200 fg/mL for MAGE-1 detection in human serum sample. By adding a layer of 3-Glycidoxypolytrimethoxysilane (3-GOPS), B. Demirbakan and M.K. Sezgintürk created an immunosensor functioning on the same principles, rendering the sensor reusable since no cross-linking agent was required (Demirbakan and Sezgintürk, 2017). Studies with human serum samples suggested that the biosensor could accurately recognize the protein using inexpensive disposable ITO electrodes instead of costly procedures like ELISA, with a relatively broad determination range of 0.5–15 fg/mL.

Silicon quantum dots (SiQDs) have been used as photoluminescence biosensors to detect LDH activity, known to catalyse the Lactate + NAD⁺ → Pyruvate + NADH + H⁺ reaction (Zhou et al., 2022). The fluorescence of SiQDs in this system was first quenched by nicotinamide adenine dinucleotide (NADH) due to NADH diffusion to the SiQDs surface, resulting in an electron transfer (ET) process, and then recovered by adding LDH, which catalytically consumed NAD. Despite the high selectivity, the linear detectable concentration range was 770–385,000 U/L, implying that the assay could be used to analyse LDH in human serum samples only as a prognostic indicator for melanoma patients.

Keum et al. developed a microneedle-based biosensor device integrated with an endomicroscope for simultaneous imaging and biosensor-based diagnosis of metastatic melanoma by detecting nitric oxide (NO) (Fig. 10a) (Keum et al., 2015). The microneedles are capable of detecting NO signals in real-time with high carrier mobility and sensitivity, allowing for the efficient detection of sub-micromolar

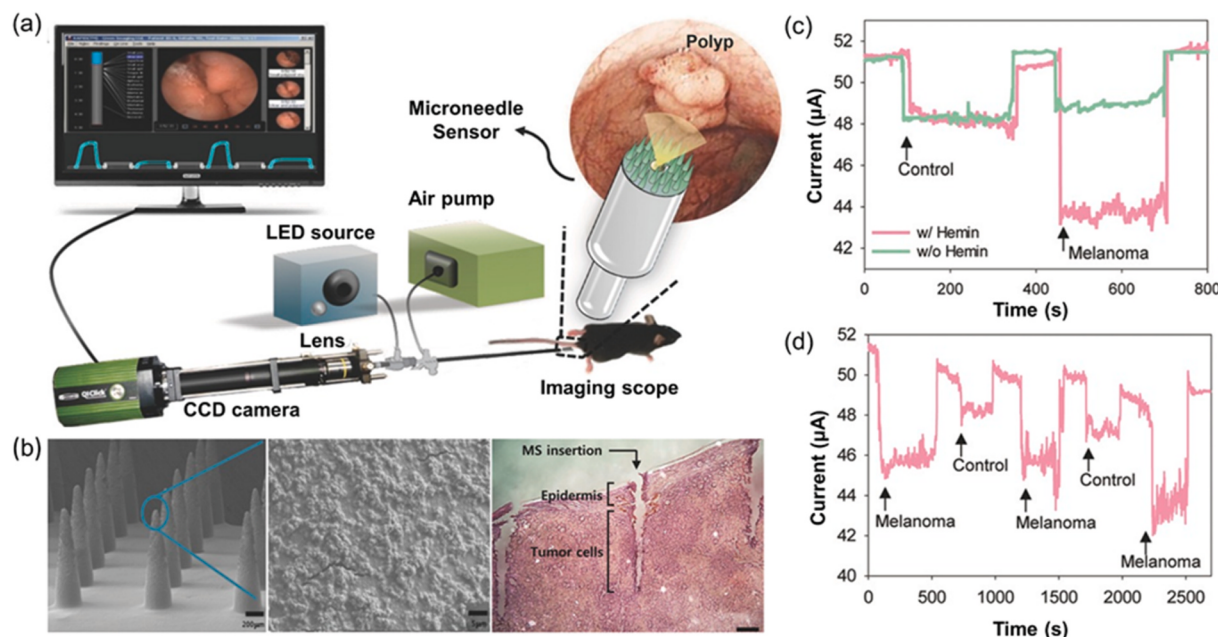


Fig. 10. Microneedle biosensor direct melanoma diagnosis during endoscopy: (a) Illustration of the microneedles at the end of the probe for in-vivo imaging of metastatic melanoma at the colon area (b) Scanning electron microscopic (SEM) images of hemin functionalized microneedle-arrays in different focus magnitudes and histological analysis of melanoma tissue after insertion of a microneedle sensor; scale bars: 200 μm , 5 μm and 100 μm (c) In vivo real-time detection of NO from melanoma tissues d) In vivo current change of the MN platform while penetrating healthy and cancerous mouse skin. [Keum et al., \(2015\)](#); Copyright © 2015 WILEY-VCH.

concentrations of NO. The electrochemical biosensor consists of a microneedle array equipped with electrodes and coated with the conducting polymer polyaniline (PANI) (Fig. 10b). It enables the diffusion of cancer cells and reaction with the immobilized NO-specific probe, resulting in a change in the electrical current in real-time. The *in vivo* dual-diagnostic device was able to distinguish the difference in NO levels between cancerous and healthy tissues in melanoma mouse skin and colon areas with a LOD of $1 \times 10^{-6} \text{ M}$, suggesting its potential as a combinational tool for melanoma diagnosis (Fig. 10c and d).

6. Summary and conclusions

Research targets non-invasive diagnosis using accessible body fluids with identified melanoma biomarkers (Belter et al., 2017; Gerloff et al., 2020). Yet, complexity and varied microenvironments hinder an optimal biomarker. Challenges include variability in collection, processing, and demographics (Friedel et al., 2023). Most biosensors focus on metastatic melanoma, but equal attention is needed for early primary melanoma detection expressed as an individualized fold-change difference. A summary of biosensors which are advancing melanoma mitigation is presented in Table 2, facilitating a critical comparison. Additionally, the emergence of wearable biosensing technologies offers a unique opportunity in this space (Yetisen et al., 2018). These wearable devices, which can monitor various physiological markers and skin conditions in real-time, have the potential to revolutionize the early detection and continuous monitoring of melanoma (Ciui et al., 2018). This review uniquely synthesizes recent breakthroughs in biosensing technologies, highlighting their transformative role in advancing melanoma diagnosis and patient care. Advances in biosensing tech offer the potential for improving medical diagnosis and treatment. Optical biosensors, often preferred for their high sensitivity and low susceptibility to interferences, have been integrated with nanomaterials for quantitative results, particularly in melanoma detection (Chai et al., 2015; Hu et al., 2017; Yang et al., 2014). Real-time and liquid biopsy methods show promise for micromelanoma detection and disease monitoring (Zambito et al., 2022). Cell signalling proteins enhance early diagnosis

and intraoperative melanoma detection, improving outcomes (Day et al., 2013). Biosensors combined with photodynamic therapy offer theragnostic benefits for melanoma care, addressing socioeconomic disparities in diagnosis and treatment (Viraka Nellore et al., 2014). Microneedles enable diagnosis and treatment at the site, and bioreceptor-transducer combinations enhance sensitivity and accuracy (Al Sulaiman et al., 2019; Keum et al., 2015; Madden et al., 2020; Yang et al., 2022). Some biosensing tech focuses on tumour identification by detecting mutations and gene overexpression in suspicious tissue samples, serving as adjunctive tools for histopathological diagnosis (Fioravanti et al., 2016; Huber et al., 2013). Others aim for a definitive diagnosis without the need for tissue samples (Demirbakan and Sezginturk, 2017; Gundogdu et al., 2017; May et al., 2005). Portable devices, including SERS and lab-on-chip systems, enable POC testing, enhancing early disease detection (Anu Prathap et al., 2019; Wang et al., 2014). These breakthroughs confirm that biosensing techniques offer significant public health benefits by increasing the accuracy of early detection cost-effectively and efficiently. The development of clinically validated end-to-end conclusive diagnostic devices using biosensing technologies holds great potential for POC melanoma diagnosis.

7. Future perspectives

Future research should explore the clinical relevance of the developed biosensors in melanoma diagnosis, treatment monitoring, and equitable healthcare access. To address disparities, a comprehensive and unbiased dataset is crucial for training AI-supported algorithms, encompassing the wide-ranging population affected by melanoma (Schlessinger et al., 2019). This effort is essential to address disparities in disease presentation and mortality rates among minority populations. In addition, the role of wearable biosensors in melanoma detection and management is an area ripe for exploration (Ciui et al., 2018). These technologies could allow for continuous, non-invasive monitoring of skin health, potentially leading to earlier detection and more personalized treatment plans. Considering the notable gap in extensive and rigorous clinical trials dedicated to biosensors for melanoma skin cancer

Table 2
Summative table of melanoma detection biosensing technologies.

	Biosensor classification	Melanoma biomarker	Detection principle	Cancer stage	Limit of detection	Ref.
Optical Biosensors	Near-infrared absorption	Spectral forms and methylene stretch ratios	Label-free detection of malignant cells	Metastatic melanoma	Qualitative result	Fioravanti et al. (2016)
	Bioluminescence	N/A	Imaging of macrophage accumulation in tumour	Metastatic melanoma	Qualitative result	Zambito et al. (2022)
	Near-infrared fluorescence	VEGF, EGFR, or IL-6R	Binding efficiency of fluorescent antibodies	Metastatic melanoma	Qualitative result	Day et al. (2013)
	Fluorescence	CDK4	Protein binding efficiency and phosphorylation in tumour cells	Not stage-specific	Qualitative result	Prevel et al. (2016)
	Fluorescent DNA biosensor	BRAF mutation	Fluorescence quenching and turn-on detection	Not stage-specific	Qualitative result	Li et al. (2016)
	Fluorescent aptamer biosensor	Melanoma CTCs	CTCs detection by the inhibitor of apoptosis	Metastatic melanoma	Qualitative result	Viraka Nellore et al. (2014)
	Immuno-magnetic biosensor	CD63-positive exosomes for Cav1 detection	CD63-positive exosomes isolation by antibodies	Primary melanoma	Qualitative result	Choi et al. (2022)
	Fluorescent imaging	Tyrosinase	Bioconjugated enzyme substrate induces fluorescence	Early stage	0 U/L	Zhan et al. (2018)
	Fluorescent imaging	Tyrosinase	Fluorescence quenching of chemical functional groups	Early stage	2 nM	Kumar et al. (2020)
	Fluorescence	Tyrosinase	Fluorescence quenching of functionalized CQDs	Not stage-specific	$7 \cdot 10^{-3}$ U/mL	Chai et al. (2015)
	Fluorescence	Tyrosinase	Fluorescence quenching of functionalized CQDs	Not stage-specific	$17.7 \cdot 10^{-3}$ U/mL	Hu et al. (2017)
	Fluorescence	Tyrosinase	Fluorescence quenching of functionalized gold NCs	Not stage-specific	0.08 U/mL	Yang et al. (2014)
	Fluorescence	Tyrosinase	Ratiometric fluorescence of glutathione-protected gold NCs	Not stage-specific	0.006 U/mL	Teng et al. (2015)
	Fluorescence	Tyrosinase	PET quenching of fluorescently bioconjugated modified gold-silver NCs	Not stage-specific	0.0135 U/mL	Ao et al. (2016)
	Fluorescence	LDH	SiQDs fluorescence quenching and electron transfer process	Not stage-specific	0.77 U/L	Zhou et al. (2022)
Electro-chemical sensors	SERS	Tyrosinase	Spectral variations on the SERS substrate	Not stage-specific	0.07 U/mL	Wang et al. (2019)
	Fluorescence	cfNAs	Signal alteration by DNA hybridization	Metastatic melanoma	6 nM	Al Sulaiman et al. (2019)
	Potentiometric	VEGF	Cell sensor with a functionalized ion-selective electrode	Metastatic melanoma	70 pg/mL	(May et al., 2005)
	Impedimetric	MAGE-1	Binding efficiency of anti-MAGE-I antibody	Not stage-specific	1.3 fg/mL	Gundogdu et al. (2017)
	Impedimetric	MAGE-1	Binding efficiency of anti-MAGE-I antibody	Not stage-specific	0.5 fg/mL	Demirbakan and Sezginerturk (2017)
	Potentiometric	BRAFV ^{600E} mutation	Antigen detection by the immobilized anti-BRAFV ^{600E} antibody	Metastatic melanoma	100 cells/mL	Wuethrich et al. (2021)
	Impedimetric	CD146	Binding efficiency of anti-CD146 antibody	Not stage-specific	3.4 pg/mL	Ren et al. (2014)
	Impedimetric	MC1R	Binding efficiency of the anti-MC1R antibody on nanofibers	Not stage-specific	1 cell/mL	Prathap et al. (2018)
	Amperometric	DOPA/Tyrosinase	pAMTA electrode combined with CV	Not stage-specific	$1.9 \cdot 10^{-10}$ M	Revin and John (2013)
	Amperometric	S100B	S100B binding efficiency to a peptide coupled with a signal peptide	Metastatic melanoma	0.1 nM	Wang et al. (2014)
Piezoelectric sensors	Amperometric	S100B	Decrease in current signal due to antigen-antibody binding	Metastatic melanoma	1.9 pg/mL	Zhang et al. (2022a)
	Amperometric	Tyrosinase	Catechol functionalized microneedles for current signal generation	Not stage-specific	0.1 mg/mL	Giui et al. (2018)
	Potentiometric	Tyrosinase	Bio-FET with self-assembled nanostructured tetrapeptide on transistors	Not stage-specific	1.9 fM	Ren et al. (2022)
	Amperometric	Melanoma CTCs	Antigen-antibody interaction hindering electron transfer	Metastatic melanoma	20 cells/mL	Seenivasan et al. (2015)
	Impedimetric	Melanoma CTCs	Immunogenic binding induced changes in the impedance	Metastatic melanoma	1 cell/mL	Anu Prathap et al. (2019)
Piezoelectric sensors	Amperometric	Nitric oxide	Electrical current upon the interaction of cancer cells with NO-probe	Metastatic melanoma	$1 \cdot 10^{-6}$ M	Keum et al. (2015)
	Piezoelectric sensors	Molecular diagnostics	BRAFV ^{600E} mutation	Primary and metastatic	25 nM	Huber et al. (2013)

detection, initiating such research is crucial. These studies must be methodically organized and inclusive, involving a broad and varied patient demographic, to facilitate the swift and effective incorporation of these advanced technologies into healthcare frameworks. Robust biosensors must be validated with clinically relevant biomarker

concentrations and combinative multiplexed biosensors consisting of panels of biomarkers for tailored diagnosis and treatment. Such validation should include studies in human samples, animal models, and adequately simulative 3D tissue-engineered melanoma models (Totti et al., 2019). Integration with mobile health tech can enhance data

analysis, sophisticated communication with healthcare providers, and provider-patient communication (Zhang et al., 2022b). Addressing cost, manufacturing, and regulatory challenges is vital (Prabowo et al., 2021). Skin biosensors promise transformative “P4 medicine” (predictive, personalized, preventative, participatory) (Flores et al., 2013), offering a solution to disparities in melanoma detection and improving treatment outcomes among minority populations (Zucolotto, 2020).

CRediT authorship contribution statement

Eleni Chatzilakou: Data curation, Formal analysis, Investigation, Methodology, Writing – original draft, Writing – review & editing. **Yubing Hu:** Supervision. **Nan Jiang:** Supervision, Writing – review & editing. **Ali K. Yetisen:** Conceptualization, Funding acquisition, Project administration, Supervision, Validation, Writing – review & editing.

Declaration of competing interest

The authors declare that they have no known competing financial interests or personal relationships that could have appeared to influence the work reported in this paper.

Data availability

No data was used for the research described in the article.

Acknowledgements

A.K.Y. acknowledges MIT-Imperial Seed Fund (CEFAC.G10289). N.J. acknowledges the National Natural Science Foundation of China (82102182), the Fundamental Research Funds for the Central Universities (YJ202152), and JinFeng Laboratory, Chongqing, China (jfkjyf202203001). E.C. acknowledges “Bio Render” for the fundamental skin structure (Fig. 2) and illustrational elements (Fig. 4) for demonstration within the manuscript.

References

- Aberg, P., Nicander, I., Hansson, J., Geladi, P., Holmgren, U., Ollmar, S., 2004. IEEE Trans. Biomed. Eng. 51 (12), 2097–2102.
- Abu Owida, H., 2022. J. Skin Cancer 2022, 2961996.
- Al Sulaiman, D., Chang, J.Y.H., Bennett, N.R., Topouzi, H., Higgins, C.A., Irvine, D.J., Ladame, S., 2019. ACS Nano 13 (8), 9620–9628.
- American Cancer Society, I., 2023. Key Statistics for Melanoma Skin Cancer.
- Anu Prathap, M.U., Castro-Perez, E., Jimenez-Torres, J.A., Setaluri, V., Gunasekaran, S., 2019. Biosens. Bioelectron. 142, 111522.
- Ao, H., Qian, Z., Zhu, Y., Zhao, M., Tang, C., Huang, Y., Feng, H., Wang, A., 2016. Biosens. Bioelectron. 86, 542–547.
- Artes Electronics Pte Ltd, 2023. NOTA Mole Tracker.
- Atkins, M.B., Curiel-Lewandrowski, C., Fisher, D.E., Swetter, S.M., Tsao, H., Aguirre-Ghiso, J.A., Soengas, M.S., Weeraratna, A.T., Flaherty, K.T., Herlyn, M., Sosman, J. A., Tawbi, H.A., Pavlick, A.C., Cassidy, P.B., Chandra, S., Chapman, P.B., Daud, A., Eroglu, Z., Ferris, L.K., Fox, B.A., Gershenwald, J.E., Gibney, G.T., Grossman, D., Hanks, B.A., Hanniford, D., Hernando, E., Jeter, J.M., Johnson, D.B., Kleif, S.N., Kirkwood, J.M., Leachman, S.A., Mays, D., Nelson, K.C., Sondak, V.K., Sullivan, R.J., Merlino, G., Melanoma Research, F., 2021. Clin. Cancer Res. 27 (10), 2678–2697.
- Avagliano, A., Fiume, G., Pelagalli, A., Sanita, G., Ruocco, M.R., Montagnani, S., Arcuolo, A., 2020 (2234-943X (Print)). Front. Oncol. 10, 722.
- Bakker, E., Telting-Diaz, M., 2002. Anal. Chem. 74 (12), 2781–2800.
- Barak, V., Leibovici, V., Peretz, T., Kalichman, I., Lotem, M., Merims, S., 2015. Anticancer Res. 35 (12), 6755–6760.
- Bauzá, P., Leemans, M., Audureau, E., Gilbert, C., Armal, C., Fromantin, I., 2022. Integr. Cancer Ther. 21, 15347354221140516.
- Belter, B., Haase-Kohn, C., Pietzsch, J., 2017. Codon Publications.
- Bhalla, N., Jolly, P., Formisano, N., Estrela, P., 2016. Essays Biochem. 60 (1), 1–8.
- Bolander, A., Agnarsson, M., Stromberg, S., Ponten, F., Hesselius, P., Uhlen, M., Bergqvist, M., 2008. Cancer Genomics Proteomics 5 (6), 293–300.
- Borsari, S., Longo, C., 2017. In: Argenziano, G., Lallas, A., Longo, C., Moscarella, E., Kyrgidis, A., Ferrara, G. (Eds.), Cutaneous Melanoma. Academic Press, pp. 81–90.
- Boussadia, Z., Lamberti, J., Mattei, F., Pizzi, E., Puglisi, R., Zanetti, C., Pasquini, L., Fratini, F., Fantozi, L., Felicetti, F., Fecchi, K., Raggi, C., Sanchez, M., D’Atri, S., Care, A., Sargiacomo, M., Parolini, I., 2018. J. Exp. Clin. Cancer Res. 37 (1), 245.
- Bouwhuis, M.G., Suciu, S., Kruit, W., Sales, F., Stoitchkov, K., Patel, P., Cocquyt, V., Thomas, J., Lienard, D., Eggermont, A.M., Ghanem, G., European Organisation for, R., Treatment of Cancer Melanoma, G., 2011. Eur. J. Cancer 47 (3), 361–368.
- Bucur, B., Purcarea, C., Andreescu, S., Vasilescu, A., 2021. Sensors 21 (9).
- Canfield Scientific Inc., 2023. Whole Body 3D Imaging.
- Carrara, M., Bono, A., Bartoli, C., Colombo, A., Lualdi, M., Moglia, D., Santoro, N., Tolomio, E., Tomatis, S., Tragni, G., Santinami, M., Marchesini, R., 2007. Phys. Med. Biol. 52 (9), 2599–2613.
- Chai, L., Zhou, J., Feng, H., Tang, C., Huang, Y., Qian, Z., 2015. ACS Appl. Mater. Interfaces 7 (42), 23564–23574.
- Choi, D.Y., Park, J.N., Paek, S.H., Choi, S.C., Paek, S.H., 2022. Biosens. Bioelectron. 198, 113828.
- Ciui, B., Martin, A., Mishra, R.K., Brunetti, B., Nakagawa, T., Dawkins, T.J., Lyu, M., Cristea, C., Sandulescu, R., Wang, J., 2018. Adv. Healthcare Mater. 7 (7), e1701264.
- D’Amico, A., Bono, R., Pennazza, G., Santonicò, M., Mantini, G., Bernabei, M., Zarlunga, M., Roscioni, C., Martinelli, E., Paolesse, R., Di Natale, C., 2008. Skin Res. Technol. 14 (2), 226–236.
- D’Orazio, J., Jarrett, S., Amaro-Ortiz, A., Scott, T., 2013. Int. J. Mol. Sci. 14 (6), 12222–12248.
- Davis, L.E., Shalin, S.C., Tackett, A.J., 2019. Cancer Biol. Ther. 20 (11), 1366–1379.
- Day, K.E., Beck, L.N., Deep, N.L., Kovar, J., Zinn, K.R., Rosenthal, E.L., 2013. Laryngoscope 123 (11), 2681–2689.
- Demirbakan, B., Sezgin, M.K., 2017. Talanta 169, 163–169.
- Desai, A.D., Chinta, S., Yeh, C., Shah, V.P., Shah, R., Paskhover, B., Schwartz, R.A., 2023. Arch. Dermatol. Res. 315 (4), 799–806.
- Diaz, M.I., Diaz, P., Bennett, J.C., Urra, H., Ortiz, R., Orellana, P.C., Hetz, C., Quest, A.F. G., 2020. Cell Death Dis. 11 (8), 648.
- Drabnerova, L., Cerna, H., Brodská, H., Boubelík, M., Watt, S.M., Stanners, C.P., Dráber, P., 2000. Immunology 101 (2), 279–287.
- Dratkiewicz, E., Simiczyjew, A., Mazurkiewicz, J., Zietek, M., Matkowski, R., Nowak, D., 2021. Cells 10 (4).
- Eftekhari, A., Ahmadian, E., Salatin, S., Sharifi, S., Dizaj, S.M., Khalilov, R., Hasanzadeh, M., 2019. TrAC, Trends Anal. Chem. 116, 122–135.
- Escors, D., 2014. New J. Sci. 2014, 734515.
- Fahmy, L.M., Schreidah, C.M., Geskin, L.J., 2023. JAAD International 11, 78–82.
- Fioravanti, V., Brandhoff, L., van den Driesche, S., Breiteneder, H., Kitzwanger, M., Hafner, C., Vellekoop, M.J., 2016. Sensors 16 (10).
- Flores, M., Glusman, G., Brogaard, K., Price, N.D., Hood, L., 2013. Per. Med. 10 (6), 565–576.
- Freeman, K., Dinnis, J., Chucho, N., Takwoingi, Y., Bayliss, S.E., Matin, R.N., Jain, A., Walter, F.M., Williams, H.C., Deeks, J.J., 2020. BMJ 368, m127.
- Friedel, M., Thompson, I.A.P., Kasting, G., Polksky, R., Cunningham, D., Soh, H.T., Heikenfeld, J., 2023. Nat. Biomed. Eng. 1–15.
- Gehring, S., Gottmann, D., Missler, U., Wiesmann, M., 1998. Clin. Chem. 44 (5), 1056–1058.
- Gerloff, D., Sunderkotter, C., Wohlrab, J., 2020. Skin Pharmacol. Physiol. 33 (5), 270–279.
- Ghanem, G., Fabrice, J., 2011. Mol. Oncol. 5 (2), 150–155.
- Gouzerh, F., Bessière, J.-M., Ujvari, B., Thomas, F., Dujon, A.M., Dormont, L., 2022. Biochim. Biophys. Acta Rev. Canc 1877 (1), 188644.
- Gray, M., Meehan, J., Ward, C., Langdon, S.P., Kunkler, I.H., Murray, A., Argyle, D., 2018. Vet. J. 239, 21–29.
- Groenendaal, W., von Basum, G., Schmidt, K.A., Hilbers, P.A., van Riel, N.A., 2010. J. Diabetes Sci. Technol. 4 (5), 1032–1040.
- Gunathilake, R., Schurer, N.Y., Shoo, B.A., Celli, A., Hachem, J.P., Crumrine, D., Sirimanna, G., Feingold, K.R., Mauro, T.M., Elias, P.M., 2009. J. Invest. Dermatol. 129 (7), 1719–1729.
- Gundogdu, A., Aydin, E.B., Sezgin, M.K., 2017. Anal. Biochem. 537, 84–92.
- Gutkowicz-Krusin, D., Elbaum, M., Jacobs, A., Keem, S., Kopf, A.W., Kamino, H., Wang, S., Rubin, P., Rabinovitz, H., Oliviero, M., 2000. Melanoma Res. 10 (6), 563–570.
- Han, S.S., Kim, M.S., Lim, W., Park, G.H., Park, I., Chang, S.E., 2018. J. Invest. Dermatol. 138 (7), 1529–1538.
- Harvey, V.M., Patel, H. Fau - Sandhu, S., Sandhu S Fau - Wallington, S.F., Wallington Sf Fau - Hinds, G., Hinds, G., 2014. (1526-2359 (Electronic)).
- Heineman, W.R., Jensen, W.B., 2006. Biosens. Bioelectron. 21 (8), 1403–1404.
- Heimann, C.W., 2019. Biochim. Biophys. Acta Mol. Cell Res. 1866 (7), 1197–1206.
- Hu, J.J., Bai, X.L., Liu, Y.M., Liao, X., 2017. Anal. Chim. Acta 995, 99–105.
- Huber, F., Lang, H.P., Backmann, N., Rimoldi, D., Gerber, C., 2013. Nat. Nanotechnol. 8 (2), 125–129.
- Hughes, A.J., Tawfik, S.S., Baruah, K.P., O’Toole, E.A., O’Shaughnessy, R.F.L., 2021. Br. J. Dermatol. 185 (1), 26–35.
- Jing, X., Michael, C.W., Theoharis, C.G., 2013. Diagn. Cytopathol. 41 (2), 126–130.
- Jung-Garcia, Y., Maiques, O., Monger, J., Rodriguez-Hernandez, I., Fanshawe, B., Domar, M.C., Renshaw, M.J., Marti, R.M., Matias-Guiu, X., Collinson, L.M., Sanz-Moreno, V., Carlton, J.G., 2023. Nat. Cell Biol. 25 (1), 108–119.
- Keereweer, S., Kerrebijn, J.D., Mol, I.M., Mieog, J.S., Van Driel, P.B., Baatenburg de Jong, R.J., Vahrmeijer, A.L., Lowik, C.W., 2012. Head Neck 34 (7), 1002–1008.
- Kensington International Clinic, 2023. Dermatology.
- Keum, D.H., Jung, H.S., Wang, T., Shin, M.H., Kim, Y.E., Kim, K.H., Ahn, G.O., Hahn, S. K., 2015. Adv. Healthcare Mater. 4 (8), 1153–1158.
- Keung, E.Z., Gershenwald, J.E., 2018. Expert Rev. Anticancer Ther. 18 (8), 775–784.
- Kim, J., Campbell, A.S., de Avila, B.E., Wang, J., 2019. Nat. Biotechnol. 37 (4), 389–406.
- Koch, A., Schwab, A., 2019. Acta Physiol. 225 (1), e13105.
- Kumar, P., Biswas, S., Koner, A.L., 2020. New J. Chem. 44 (26), 10771–10775.

- Li, C., Liu, J., Jiang, L., Xu, J., Ren, A., Lin, Y., Yao, G., 2021. Medicine (Baltimore) 100 (8), e24840.
- Li, P., He, H., Wang, Z., Feng, M., Jin, H., Wu, Y., Zhang, L., Zhang, L., Tang, X., 2016. Anal. Chem. 88 (1), 883–889.
- Lian, Y., Meng, L., Ding, P., Sang, M., 2018. Clin. Epigenet. 10 (1), 115.
- Lichtenberg, J.Y., Ling, Y., Kim, S., 2019. Sensors 19 (11).
- Linares, M.A., Zakaria, A., Nizran, P., 2015. Prim. Care 42 (4), 645–659.
- Liu, G., 2021. Front. Bioeng. Biotechnol. 9, 707615.
- Liu, H., Ge, J., Ma, E., Yang, L., 2019. Biomaterials in Translational Medicine, pp. 213–255.
- Logozzi, M., De Milito, A., Lugini, L., Borghi, M., Calabro, L., Spada, M., Perdicchio, M., Marino, M.L., Federici, C., Iessi, E., Brambilla, D., Venturi, G., Lozupone, F., Santinami, M., Huber, V., Maio, M., Rivoltini, L., Fais, S., 2009. PLoS One 4 (4), e5219.
- Madden, J., O'Mahony, C., Thompson, M., O'Riordan, A., Galvin, P., 2020. Sensing and Bio-Sensing Research 29, 100348.
- Malekzad, H., Zangabad, P.S., Mirshekari, H., Karimi, M., Hamblin, M.R., 2017. Nanotechnol. Rev. 6 (3), 301–329.
- Malvehy, J., Pellaconi, G., 2017. Acta Derm. Venereol. Suppl. 218, 22–30.
- Markel, G., Ortenberg, R., Seidman, R., Sapoznik, S., Koren-Morag, N., Besser, M.J., Bar, J., Shapira, R., Kubi, A., Nardini, G., Tessone, A., Treves, A.J., Winkler, E., Orenstein, A., Schachter, J., 2010. Cancer Immunol. Immunother. 59 (2), 215–230.
- Matichard, E., Verpillat, P., Meziani, R., Gerard, B., Descamps, V., Legroux, E., Burnouf, M., Bertrand, G., Bouscarat, F., Archimbaud, A., Picard, C., Ollivaud, L., Basset-Seguin, N., Kerob, D., Lanterrier, G., Lebbe, C., Crickx, B., Grandchamp, B., Soufri, N., 2004. J. Med. Genet. 41 (2), e13.
- May, K.M., Vogt, A., Bachas, L.G., Anderson, K.W., 2005. Anal. Bioanal. Chem. 382 (4), 1010–1016.
- McQuade, J.L., Daniel, C.R., Hess, K.R., Mak, C., Wang, D.Y., Rai, R.R., Park, J.J., Haydu, L.E., Spencer, C., Wongchenko, M., Lane, S., Lee, D.Y., Kaper, M., McKean, M., Beckermann, K.E., Rubinstein, S.M., Rooney, I., Musib, L., Budha, N., Hsu, J., Nowicki, T.S., Avila, A., Haas, T., Puligandla, M., Lee, S., Fang, S., Wargo, J., A., Gershenson, J.E., Lee, J.E., Hwu, P., Chapman, P.B., Sosman, J.A., Schadendorf, D., Grob, J.J., Flaherty, K.T., Walker, D., Yan, Y., McKenna, E., Legos, J.J., Carlino, M.S., Ribas, A., Kirkwood, J.M., Long, G.V., Johnson, D.B., Menzies, A.M., Davies, M.A., 2018. Lancet Oncol. 19 (3), 310–322.
- Merimsky, O., Shoenfeld, Y., Fishman, P., 1999. The Decade of Autoimmunity, pp. 261–267.
- MetaOptima Technology Inc., 2023. DermEngine.
- Mim, Mme, 2018. Secondary Form of Melanoma in Lymphnode ultrasound.
- Nagel, B., Dellweg, H., Giersch, L.M., 1992. Pure Appl. Chem. 64 (1), 143–168.
- Narayananamurthy, V., Padmapriya, P., Noorasafrin, A., Pooja, B., Hema, K., Firuz Khan, A.Y., Nithyakalyani, K., Samsuri, F., 2018. RSC Adv. 8 (49), 28095–28130.
- Naresh, V., Lee, N., 2021. Sensors 21 (4).
- National Cancer Institute, 2022. Five-Year Survival Rates.
- Neagu, M., Constantin, C., Cretoiu, S.M., Zurac, S., 2020. Front. Cell Dev. Biol. 8, 71.
- Palmer, S.R., Erickson, L.A., Ichetovkin, I., Knauer, D.J., Markovic, S.N., 2011. Mayo Clin. Proc. 86 (10), 981–990.
- Perez-Jimenez, A.I., Lyu, D., Lu, Z., Liu, G., Ren, B., 2020. Chem. Sci. 11 (18), 4563–4577.
- Perumal, V., Hashim, U., 2014. J. Appl. Biomed. 12 (1), 1–15.
- Prabowo, B.A., Cabral, P.D., Freitas, P., Fernandes, E., 2021. Chemosensors 9 (11).
- Prathap, M.U.A., Rodriguez, C.I., Sadak, O., Guan, J., Setaluri, V., Gunasekaran, S., 2018. Chem. Commun. 54 (7), 710–714.
- Prelvel, C., Pellerano, M., Gonzalez-Vera, J.A., Henri, P., Meunier, L., Vollaire, J., Josserand, V., Morris, M.C., 2016. Biosens. Bioelectron. 85, 371–380.
- Qi, H., Zhang, C., 2020. Anal. Chem. 92 (1), 524–534.
- Raposo, P.D., Correia, J.D., Oliveira, M.C., Santos, I., 2010. Biopolymers 94 (6), 820–829.
- Rasooly, A., Herold, K.E., 2009. Biosensors and Biodetection 2, 464.
- Rayner, J.E., Laino, A.M., Nufer, K.L., Adams, L., Raphael, A.P., Menzies, S.W., Soyer, H.P., 2018. Front. Med. 5, 152.
- Redondo, P., Bandres, E., Solano, T., Okroujnov, I., Garcia-Foncillas, J., 2000. Cytokine 12 (4), 374–378.
- Ren, H., Xu, T., Liang, K., Li, J., Fang, Y., Li, F., Chen, Y., Zhang, H., Li, D., Tang, Y., Wang, Y., Song, C., Wang, H., Zhu, B., 2022. iScience 25 (1), 103673.
- Ren, X., Yan, T., Zhang, Y., Wu, D., Ma, H., Li, H., Du, B., Wei, Q., 2014. Biosens. Bioelectron. 58, 345–350.
- Revin, S.B., John, S.A., 2013. Sens. Actuators B Chem. 188, 1026–1032.
- Riechers, A., Bosscherhoff, A.K., 2014. Exp. Dermatol. 23 (1), 12–14.
- Rigel, D.S., Russak, J., Friedman, R., 2010. CA cancer. J. Clin. 60 (5), 301–316.
- Rodrigues, D., Barbosa, A.I., Rebelo, R., Kwon, I.K., Reis, R.L., Correlo, V.M., 2020. Biosensors 10 (7).
- Rosenkranz, A.A., Slastnikova, T.A., Durymanov, M.O., Sobolev, A.S., 2013. Biochemistry (Mosc.) 78 (11), 1228–1237.
- Saginala, K., Barsouk, A., Aluru, J.S., Rawla, P., Barsouk, A., 2021. Med. Sci. 9 (4), 139–149.
- Sahu, P., Kashaw, S.K., Sau, S., Kushwah, V., Jain, S., Agrawal, R.K., Iyer, A.K., 2019. Int. J. Biol. Macromol. 128, 740–751.
- Salazar-Onfray, F., Lopez, M., Lundqvist, A., Aguirre, A., Escobar, A., Serrano, A., Korenblit, C., Petersson, M., Chhajlani, V., Larsson, O., Kiessling, R., 2002. Br. J. Cancer 87 (4), 414–422.
- Samant, P.P., Niedzwiecki, M.M., Raviele, N., Tran, V., Mena-Lapaix, J., Walker, D.I., Felnier, E.I., Jones, D.P., Miller, G.W., Prausnitz, M.R., 2020. Sci. Transl. Med. 12 (571).
- Samant, P.P., Prausnitz, M.R., 2018. Proc. Natl. Acad. Sci. U. S. A. 115 (18), 4583–4588.
- Scheepers, M., Al-Difaie, Z., Brandts, L., Peeters, A., van Grinsven, B., Bouvy, N.D., 2022. JAMA Netw. Open 5 (6), e2219372.
- Schlessinger, D.I., Chhor, G., Gevaert, O., Swetter, S.M., Ko, J., Novoa, R.A., 2019. Semin. Cutan. Med. Surg. 38 (1), E31–E37.
- Seenivasan, R., Maddodi, N., Setaluri, V., Gunasekaran, S., 2015. Biosens. Bioelectron. 68, 508–515.
- Senf, B., Yeo, W.H., Kim, J.H., 2020. Biosensors 10 (9).
- Shao, K., Feng, H., 2022. J Clin. Aesthet. Dermatol. 15 (7), 16–22.
- Sonesson, B., Eide, S., Ringborg, U., Rorsman, H., Rosengren, E., 1995. Melanoma Res. 5 (2), 113–116.
- Stoitchkov, K., Letellier, S., Garnier, J.P., Bousquet, B., Tsankov, N., Morel, P., Ghanem, G., Le Bricon, T., 2002. Melanoma Res. 12 (3), 255–262.
- Strategic Market Search, 2022. POC Diagnostic Biosensors Market Size, Trends and Growth Analysis, Forecast, pp. 2021–2030.
- Tagliabue, E., Gandini, S., Bellocchio, R., Maisonneuve, P., Newton-Bishop, J., Polksky, D., Lazovich, D., Kanetsky, P.A., Ghiorzo, P., Gruis, N.A., Landi, M.T., Menin, C., Farnoli, M.C., Garcia-Borrón, J.C., Han, J., Little, J., Sera, F., Raimondi, S., 2018, 1179–1322 (Print). Cancer Manag. Res. 10, 1143–1154.
- Tainaka, K., Sakaguchi, R., Hayashi, H., Nakano, S., Liew, F.F., Morii, T., 2010. Sensors 10 (2), 1355–1376.
- Teng, Y., Jia, X., Li, J., Wang, E., 2015. Anal. Chem. 87 (9), 4897–4902.
- The Human Protein Atlas, 2022a. Melan-A - the Human Protein Atlas.
- The Human Protein Atlas, 2022b. Melanocyte Inducing Transcription Factor- the Human Protein Atlas.
- The Human Protein Atlas, 2022c. Premelanosome Protein-The Human Protein Atlas.
- The Human Protein Atlas, 2022d. S100 Calcium Binding Protein B- the Human Protein Atlas.
- The Insight Partners, 2022a. Global Skin Cancer Diagnostics Market, Global Skin Cancer Diagnostics Market.
- The Insight Partners, 2022b. Skin Cancer Diagnostics Market Size Worth \$5.48Bn. Bloomberg. Globally, by 2028 at 7.2% CAGR.
- Thompson, G., 2023. Lentigo Maligna (LM) on the Temple.
- Tognetti, L., Fiorani, D., Tonini, G., Zuliani, L., Cataldo, G., Balistreri, A., Cevenini, G., Cinotti, E., Rubegni, P., 2020. In: Fimiani, M., Rubegni, P., Cinotti, E. (Eds.), Technology in Practical Dermatology: Non-invasive Imaging, Lasers and Ulcer Management. Springer International Publishing, Cham, pp. 3–24.
- Totti, S., Ng, K.W., Dale, L., Lian, G., Chen, T., Velliou, E.G., 2019. Sens. Actuators B Chem. 296, 126652.
- Trager, M.H., Geskin, L.J., Samie, F.H., Liu, L., 2022. Exp. Dermatol. 31 (1), 4–12.
- Tschandl, P., 2018. (2160-9381 (Print)).
- Tschandl, P., Codella, N., Akay, B.N., Argenziano, G., Braun, R.P., Cabo, H., Gutman, D., Halpern, A., Helba, B., Hofmann-Wellenhof, R., Lallas, A., Lapins, J., Longo, C., Malvehy, J., Marchetti, M.A., Marghoob, A., Menzies, S., Oakley, A., Paoli, J., Puig, S., Rinner, C., Rosendahl, C., Scope, A., Sinz, C., Soyer, H.P., Thomas, L., Zalaudek, I., Kittler, H., 2019. Lancet Oncol. 20 (7), 938–947.
- Undén, J., Bellner, J., Eneroth, M., Alling, C., Ingebrigtsen, T., Romner, B., 2005. J. Trauma Acute Care Surg. 58 (1).
- Vaupel, P., Kallinowski, F., Okunieff, P., 1989. Cancer Res. 49 (23), 6449–6465.
- Velusamy, V., Arshak, K., Korostynska, O., Oliwa, K., Adley, C., 2010. Biotechnol. Adv. 28 (2), 232–254.
- Viraka Nellore, B.P., Pramanik, A., Chavva, S.R., Sinha, S.S., Robinson, C., Fan, Z., Kanchanapally, R., Grennell, J., Weaver, I., Hamme, A.T., Ray, P.C., 2014. Faraday Discuss. 175, 257–271.
- Vo-Dinh, T., Cullum, B., 2000. Fresenius' J. Anal. Chem. 366 (6–7), 540–551.
- Wagner, N.B., Weide, B., Gries, M., Reith, M., Tarnanidis, K., Schuermans, V., Kemper, C., Kehrel, C., Funder, A., Lichtenberger, R., Sucker, A., Herpel, E., Holland-Letz, T., Schadendorf, D., Garbe, C., Umansky, V., Utikal, J., Gebhardt, C., 2019. J. Immunother. Cancer 7 (1), 343.
- Waldman, R.A., Grant-Kels, J.M., Curiel, C.N., Curtis, J., Rodriguez, S.G., Hu, S., Kerr, P., Marghoob, A., Markowitz, O., Pellacani, G., Rabinovitz, H., Rao, B., Scope, A., Stein, J.A., Swetter, S.M., 2021. J. Am. Acad. Dermatol. 85 (3), 745–749.
- Wang, L., Gan, Z.F., Guo, D., Xia, H.L., Patrice, F.T., Hafez, M.E., Li, D.W., 2019. Anal. Chem. 91 (10), 6507–6513.
- Wang, X., Li, H., Li, X., Chen, Y., Yin, Y., Li, G., 2014. Electrochim. Commun. 39, 12–14.
- Weedon, D., 2010. Weedon's Skin Pathology, third ed. 709-756.e761.
- Weinstein, D., Leininger, J., Hamby, C., Safai, B., 2014. J. Clin. Aesthet. Dermatol. 7 (6), 13–24.
- Wikipedia, E., Siascope, a Melanoma Screening Device.
- Williams, H., Pembroke, A., 1989. Lancet 333 (8640), 734.
- Willis, C.M., Britton, L.E., Swindells, M.A., Jones, E.M., Kemp, A.E., Muirhead, N.L., Gul, A., Matin, R.N., Knutsson, L., Ali, M., 2016. Br. J. Dermatol. 175 (5), 1020–1029.
- Wisniewski, N., Reichert, M., 2000. Colloids Surf. B Biointerfaces 18 (3–4), 197–219.
- Wong, R., Tran, V., Talwalker, S., Benson, N.R., 2006. J. Dermatol. Sci. 44 (2), 81–92.
- World Health Organization, 2020. Estimated Number of Deaths from 2020 to 2040, Mortality, Both Sexes, Age [0-85+]. Cancer Tomorrow International Agency for Research on Cancer.
- Wuetrich, A., Dey, S., Koo, K.M., Sina, A.A.I., Trau, M., 2021. In: Hargadon, K.M. (Ed.), Melanoma: Methods and Protocols. Springer US, New York, NY, pp. 265–276.
- Yang, J., Yang, J., Gong, X., Zheng, Y., Yi, S., Cheng, Y., Li, Y., Liu, B., Xie, X., Yi, C., Jiang, L., 2022. Adv. Healthcare Mater. 11 (10), e2102547.
- Yang, X., Luo, Y., Zhuo, Y., Feng, Y., Zhu, S., 2014. Anal. Chim. Acta 840, 87–92.
- Yetisen, A.K., Martinez-Hurtado, J.L., Unal, B., Khademhosseini, A., Butt, H., 2018. Adv. Mater. 30 (33), e1706910.

- Yetisen, A.K., Moreddu, R., Seifi, S., Jiang, N., Vega, K., Dong, X., Dong, J., Butt, H., Jakobi, M., Elsner, M., Koch, A.W., 2019. *Angew Chem. Int. Ed. Engl.* 58 (31), 10506–10513.
- Young, A.T., Vora, N.B., Cortez, J., Tam, A., Yeniyay, Y., Afifi, L., Yan, D., Nosrati, A., Wong, A., Johal, A., Wei, M.L., 2021. *Pigment Cell Melanoma Res* 34 (2), 288–300.
- Young, A.T., Xiong, M., Pfau, J., Keiser, M.J., Wei, M.L., 2020. *J. Invest. Dermatol.* 140 (8), 1504–1512.
- Zambito, G., Mishra, G., Schliehe, C., Mezzanotte, L., 2022. *Front. Bioeng. Biotechnol.* 10, 867164.
- Zhan, C., Cheng, J., Li, B., Huang, S., Zeng, F., Wu, S., 2018. *Anal. Chem.* 90 (15), 8807–8815.
- Zhang, H., Qu, H., Cui, J., Duan, L., 2022a. *RSC Adv.* 12 (40), 25844–25851.
- Zhang, S., Chen, K., Liu, H., Jing, C., Zhang, X., Qu, C., Yu, S., 2021. *J. Immunother.* 44 (6), 214–223.
- Zhang, Y., Hu, Y., Jiang, N., Yetisen, A.K., 2022b. *Biosens. Bioelectron.* 219, 114825.
- Zhou, Y., Qi, M., Yang, M., 2022. *Spectrochim. Acta Mol. Biomol. Spectrosc.* 268, 120697.
- Ziegler, C., 2000. *Fresenius' J. Anal. Chem.* 366 (6–7), 552–559.
- Zucolotto, V., 2020. *Frontiers in Sensors* 1.



Eleni Chatzilakou is a Ph.D. candidate in the Department of Chemical Engineering of Imperial College London and aims to develop biosensing technologies for point-of-care diagnosis of skin cancer. She holds a MEng in Chemical Engineering from the Aristotle University of Thessaloniki, during which she developed biopolymer-based scaffolds for tissue engineering applications. She has worked for the Spanish National Research Council, the National Centre of Scientific Research of Greece “Demokritos”, as well as for the pharmaceutical company “Pharmathen S.A.”.



Dr. Yubing Hu is a Research Associate and Assistant Ph.D. supervisor in the Department of Chemical Engineering at Imperial College London. Dr. Hu received a bachelor's degree from Zhejiang University in 2016 and earned a Ph.D. degree from the Hong Kong University of Science and Technology in 2020. She is experienced in organic synthesis, functional polymer materials, optical sensing and analytical devices. With an aim to innovate healthcare technologies and translate them to individualized medications, she is highly motivated to develop optical biosensors and biomedical devices for portable, wearable and implantable diagnostics and therapeutics.



Dr. Nan Jiang is a Professor of Biomedical Engineering in the West China School of Basic Medical Sciences & Forensic Medicine at Sichuan University, China. After her PhD study at Wuhan University of Technology, she worked as a postdoctoral fellow and a research associate at Harvard University and Imperial College London. Her research is aimed at optical biomedical sensors, 3D bioprinting, and microfluidic devices. She has published many papers as the first author and corresponding author in high-level journals. She has also received awards, such as “IAAM Young Scientist Medal”, “Excellence in Innovation” etc.



Dr. Ali K. Yetisen is a Senior Lecturer and Associate Professor in the Department of Chemical Engineering at Imperial College London. He was previously a Tosteson fellow at Harvard University. He holds a Ph.D. degree in Chemical Engineering and Biotechnology from the University of Cambridge. He aims to develop biochemical sensors, optical materials and devices for application in medical diagnostics, therapeutics, and imaging. He has been awarded several international prizes including the IChemE Nicklin Medal, Birmingham Fellowship, MGH ECOR Award, Humboldt Research Fellowship, Carl Friedrich von Siemens Fellowship, and Fellowship of the Royal Society of Chemistry, Fellowship of the Institute of Physics, and Fellowship of the Institution of Chemical Engineers.